REPORT DOCUMENTATION PAGE

Form Approved
OMB No. 0704-0188

1. AGENCY USE ONLY (Leave blank)	2. REPORT DATE	3. REPORT TYPE AND DATES COVERED
	August 1998	Final 10/1/94 to 3/31/98

4. TITLE AND SUBTITLE
THE IMPACT OF MICROBIOLOGICALLY INFLUENCED CORROSION ON PROTECTIVE POLYMER COATINGS

5. FUNDING NUMBERS
N00014-94-1-0026

6. AUTHOR(S)
F. Mansfeld, C.C. Lee, L.T. Han, G. Zhang, B. Little, P. Wagner, R. Ray, J. Jones-Meehan

7. PERFORMING ORGANIZATION NAME(S) AND ADDRESS(ES)
University of Southern California
Materials Science and Engineering Department
University Park, VHE 602
Los Angeles, CA 90089-0241

8. PERFORMING ORGANIZATION REPORT NUMBER
4

9. SPONSORING/MONITORING AGENCY NAME(S) AND ADDRESS(ES)
Office of Naval Research
800 N. Quincy Street
Arlington, VA 22217-5660
Attn: Code 3310

10. SPONSORING/MONITORING AGENCY REPORT NUMBER

11. SUPPLEMENTARY NOTES

12a. DISTRIBUTION/AVAILABILITY STATEMENT
Unrestricted

12b. DISTRIBUTION CODE

13. ABSTRACT (Maximum 200 words)

Mild steel panels protected with twelve different polymer coating systems have been exposed to natural seawater (NS) at Port Hueneme, CA and Key West, FL and to artificial seawater (AS) in laboratory tests. Coating performance was monitored using electrochemical impedance spectroscopy (EIS) and electrochemical noise analysis (ENA) as well as visual observations. Statistical analyses have been performed to determine the effects of coating composition on coating performance in general and attack by microorganisms in particular. After exposure to NS the test panels have been evaluated using an environmental scanning electron microscope (ESEM) to determine spatial relationships between coating damage and bacterial colonization. Exposure results for coated panels with intentional defects demonstrated that bacteria did not colonize exposed surfaces under cathodic protection. Laboratory studies were performed for panels exposed to mixed communities of bacteria containing SRB.

14. SUBJECT TERMS
polymer coatings, coating degradation, natural seawater, microorganisms, EIS, ENA, ESEM, surface analysis

15. NUMBER OF PAGES

16. PRICE CODE

17. SECURITY CLASSIFICATION OF REPORT	18. SECURITY CLASSIFICATION OF THIS PAGE	19. SECURITY CLASSIFICATION OF ABSTRACT	20. LIMITATION OF ABSTRACT

THE IMPACT OF MICROBIOLOGICALLY INFLUENCED CORROSION ON PROTECTIVE POLYMER COATINGS

F. Mansfeld, C. C. Lee, L. T. Han and G. Zhang
Corrosion and Environmental Effects Laboratory (CEEL)
Department of Materials Science and Engineering
University of Southern California
Los Angeles, CA 90089-0241

B. J. Little, P. Wagner and R. Ray
Naval Research Laboratory
Code 7333
Stennis Space Center, MS 39529-5004

J. Jones-Meehan
Naval Research Laboratory
Code 6115
Washington, DC 20175-5320

AUGUST 1998

Final Report to the Office of Naval Research
Contract No. N00014-94-1-0026

TABLE OF CONTENTS

ABSTRACT

Mild steel panels protected with twelve different polymer coating systems have been exposed to natural seawater (NS) at Port Hueneme, CA and Key West, FL and to artificial seawater (AS) in laboratory tests. Coating performance was monitored using electrochemical impedance spectroscopy (EIS) and electrochemical noise analysis (ENA) as well as visual observations. Statistical analyses have been performed to determine the effects of coating composition on coating performance in general and attack by microorganisms in particular. After exposure to NS the test panels have been evaluated using an environmental scanning electron microscope (ESEM) to determine spatial relationships between coating damage and bacterial colonization. Exposure results for coated panels with intentional defects demonstrated that bacteria did not colonize exposed surfaces under cathodic protection. Laboratory studies were performed for panels exposed to mixed communities of bacteria containing SRB.

Keywords: polymer coatings, coating degradation, natural seawater, microorganisms, EIS, ENA, ESEM, surface analysis.

1.0. INTRODUCTION

Corrosion protection by polymer coatings is one of the most common methods of corrosion control. In 1982, the total value of paints, varnishes and lacquers produced in the United States amounted to about seven billion $, half of which is estimated to be used for corrosion protection. An added cost is the labor cost of application equaling two or three times the cost of the paint. Naval vessels require four coats of paint for exterior exposures and two coats for interior surfaces, each coat on a 1600-ton destroyer requiring 1.5 tons of paint. While the factors responsible for degradation of protective polymer coatings in most environments have been studied in great detail, not much information is available at present concerning the destructive attack of bacteria in seawater on typical naval coating systems.

The impact of microorganisms on corrosion protection by polymer coatings has been evaluated for twelve coating systems on mild steel during exposure to natural seawater (NS) at Port Hueneme (PH), California and Key West (KW), Florida. For comparison, additional laboratory tests were performed in artificial seawater (AS). Coating performance was evaluated by analysis of impedance spectra and electrochemical noise data. Electrochemical impedance spectroscopy (EIS) is a powerful non-destructive tool for evaluation of coating properties and their changes with exposure time. The application of electrochemical noise analysis (ENA) to polymer coatings is relatively new. Much progress has been made in understanding of the application of ENA to the study of polymer coating degradation in this project.

Since impedance and noise measurements had to be performed for a large number of samples at the remote test sites at PH and KW, it was necessary to develop a new approach for monitoring coating properties [1-4]. Experiments were performed by an on-site computer connected to the electrochemical equipment and controlled via modem by a computer system at the Corrosion and Environmental Effects Laboratory at USC (CEEL/USC) using software developed for this purpose.

Coating degradation due to microorganisms in seawater has been determined for two coating systems. In the CR series, different primers, midcoats and topcoats have been applied. The coating systems were designed to allow evaluation of corrosion protection provided by different primers, midcoats and topcoats by comparing coating systems which differ only in one of these parameters. Results for the early stages of exposure have been discussed in previous reports [1,2]. The JJ series of coatings was designed to allow evaluation of the effects of different primers (metallic zinc, IVD aluminum and phosphate) and an additional polyurethane topcoat over an epoxy polyamide midcoat on coating performance in general and attack by microorganisms in particular. The nature of the metallic primer changes the potential of the steel/coating system and might affect interactions with microorganisms. The relationship between colonization by bacteria and defects in polymer coatings was further studied by exposure of coated samples with intentional defects in the coating. One set of these samples was exposed under cathodic protection provided by a strip of zinc.

Coated steel samples were removed from AS and NS when the rusted area exceeded 0.1 - 0.3% of the total area as determined by visual observation according to ASTM D 610. Samples removed from NS were subjected to analysis with an environmental scanning electron microscope (ESEM) to determine biofilm distribution and spatial relationships between coating damage and microorganisms.

The impact of three marine, mixed communities containing sulfate-reducing bacteria (SRB) on coating performance was studied in laboratory experiments. After different exposure

periods coating properties were evaluated with EIS [1-3]. Exposed samples were also analyzed with ESEM.

Results of 3 - 4 years exposures at PH and at KW have provided a large amount of information concerning collection of electrochemical impedance and noise data from remote test sites, analysis of impedance data for different types of coatings systems as well as analysis of noise data in the time and frequency domains. Results and interpretation have been discussed in a number of publications and presentations at technical meetings. A detailed discussion of the experimental data and their analysis will be given in this final report.

2.0. EXPERIMENTAL APPROACH

2.1. Materials and Methods

2.1.1. Materials. Two sets of coating systems (JJ and CR series) were applied on mild steel and exposed to NS at Port Hueneme, CA (PH) and Key West, FL (KW) and to AS in laboratory tests at CEEL, USC. Coating compositions and the appropriate specifications for coating application are given in Table I. For both CR and JJ coatings different primers, midcoats and topcoats were used to evaluate their effects on corrosion protection in general and attack by microorganisms in particular. In the JJ series, all coatings had an epoxy polyamide midcoat, but samples JJ2, JJ4 and JJ6 had an additional polyurethane topcoat (Table I). CR9 and JJ7 had the same coating composition, but were prepared by different vendors using different version of the appropriate MIL spec (Table I). Coating properties have been discussed in more detail in previous annual reports [1-3].

2.1.2. Methods. EIS and EN data were measured using a two-electrode arrangement for simultaneous collection of potential and current noise. At the two remote marine test sites data collection was performed under computer control via commercial telephone line to the computer at CEEL/USC [1-8]. Standard equipment was used in laboratory tests. Impedance spectra were recorded once a week, while EN data were measured twice a week. Visual rating according to ASTM D 610 was performed once a month for test samples exposed in AS and in NS (PH), and once at KW after immersion for 4 months. Samples were removed at PH and in the laboratory (AS) when the visual rating according to ASTM D 610 had dropped below 8 (0.1% rusted area). Information about first immersion and removal dates for these degraded samples was provided in a previous annual report [3]. All samples were removed from PH in October 1996 due to the closure of the seawater laboratory. All electrochemical measurements for coated samples exposed in the laboratory were terminated in July 1997. Severely degraded polymer samples in KW were removed in September 1996 and measurements were continued on the remaining sample pairs until September 1997.

Selected samples removed from AS were evaluated with a scanning Kelvin probe (Corrosion Potential Measurement System, UBM Corp., Sunnyvale, CA) to determine the potential distribution at the steel/coating interface. In this technique, an electronically conducting material, i. e. the Kelvin probe, is used to determine the work function of a material.. Suitable calibration allows conversion of the Volta potential difference between the probe tip (a fine Ni-Cr wire) and the test sample into the corrosion potential of the test sample [23,24]. The advantage of the Kelvin probe technique is the possibility to detect areas of coating delamination based on the potential distribution at the metal surface under a polymer coating.

Additional field and laboratory experiments were designed to evaluate the relationships between marine bacteria and surface defects in polymer coatings applied to mild steel.

Samples of the JJ series with intentional defects were immersed at KW with and without coupling to galvanized steel and corrosion potential (E_{corr}) and EN data were collected twice a week for 30 days. Four 0.32 cm diameter holes were drilled (two per side) 2.54 cm from the bottom edge and 2.54 cm from the side edge through the coating to create a defined holiday (Fig. 1). All samples were examined using light microscopy and ESEM coupled with energy dispersive x-ray spectroscopy (EDS) after removal from NS.

In laboratory experiments coupons from the CR series and the JJ series were exposed to different marine communities containing SRB for different time periods. Coupons were sealed in sterile Whirl-Pak bags. Postgate medium with 3.2% NaCl, 3.7 mM phosphate and lactate as the sole carbon source was added so that coupons were only submerged halfway in the growth medium. Coated coupons exposed to sterile medium only (no added bacteria) were used as controls. The marine microbial communities containing SRB included isolates from a five-step iron phosphate coated steel coupon 1(P14), a zinc plate exposed in a constant marine immersion flume tank (49Z) and an isolate from the seawater piping system of a surface ship (CG59). All Whirl-Pak bags were incubated anaerobically at room temperature. At the end of each exposure period surface topography and chemistry were documented using ESEM. The same procedure was used for JJ series coupons with attached zinc anodes.

Samples removed from all exposure sites were shipped to NRL, Stennis Space Center, MS for examination with ESEM. Wet coupons were photographed using a Polaroid CU-5 Land Camera. Each wet coupon was examined with a Wild Heerbrugg M8 zoom stereo microscope. Under the zoom stereo microscope areas of interest, including holidays, delamination, blisters, corrosion spots and stains were photographed with a Polaroid MicroCam attachment. Photographs were later used as guides to find areas of interest. Mild steel coupons from the NS exposures were transferred to separate containers of 4% glutaraldehyde (GA) in 0.45 μm filtered PH or KW NS as appropriate, used as a fixative for bacteria and microalgae, and refrigerated overnight. Mild steel coupons from laboratory exposures were also transferred to a separate container of 4% GA in AS and refrigerated overnight. Prior to microscopic examination, each coupon was removed from GA and gently rinsed in distilled water.

Wet coupons were transferred to a refrigerated Peltier cooling device maintained at 4° C and imaged in a water vapor environment at 4-5 torr in a partially hydrated state. The microscope was operated at 20 keV using the environmental secondary detector. Periodically the ESEM chamber vapor pressure was increased to 6 torr to "flood" the cooled surface with water vapor, causing condensation on the surface and fully rehydrating the sample.

2.2. Data Analysis

2.2.1. EIS data. Analysis of EIS data for coated samples has been elsewhere [1-3], where the impedance spectra were fitted to appropriate equivalent circuit (EC) models and the resulting fit parameters were discussed. Based on these analyses the extent of coating degradation was determined and attempts were made to evaluate the effects of exposure medium and coating formulation on corrosion protection of steel exposed to NS. The degree of coating degradation is based on the delaminated area (A_d) and its increase with exposure time. The delaminated area ratio (D) has been defined as $D = A_d / A$, where A is the total immersed area of the coated sample. A_d was calculated using the breakpoint frequency (f_b), defined as the frequency where the phase angle equals -45°, and results of visual rating. The relationship between f_b and A_d has been discussed by Mansfeld et al. and

other authors [9-12]. Experimental values of f_b can be normalized based on visual rating data at a certain exposure time and the time dependence of D can then be calculated for subsequent exposure times. The quantitative relationship between f_b and D was determined when the visual rating number was less than 8, i.e., D exceeded 0.1%. Since only one visual rating was performed at KW, the normalization relationship was assumed to be the same as that for PH for the same coating type. Normalization relations for a given coating were found to be very similar for AS and NS (PH). Normalization of f_b data has been performed for CR2, CR5, CR6, CR7, JJ3, JJ4 and JJ7 samples. For CR9 samples no degradation was observed during the entire exposure period. For CR1 asymmetric behavior was observed in NS and AS, i.e., one sample in the two-electrode arrangement degraded continuously, while for the other sample very little coating damage was detected. The asymmetry model [25] was used to analyze the EIS data in this case. The f_b values for CR1 were calculated using $f_b = (2\pi R_1 C_1)^{-1}$, where R_1 and C_1 are fit parameters extracted from impedance spectra related to the sample with the poor performance. The normalization relationship was established between f_b and the visual rating values for the sample with poorer performance.

For JJ1 and JJ2 with a metallic zinc primer as well as JJ5 and JJ6 with an IVD Al primer acting as sacrificial anode, visual rating data to determine A_d from f_b data were not available since rusting did not occur. For JJ5, A_d was determined from the relationship $R_p^o = R_p \cdot A_d$ ($ohm \cdot cm^2$) [13], where R_p is the polarization resistance of the area at the metal/coating interface at which coating delamination and corrosion occur and R_p^o is the specific polarization resistance of the bare metal in the same medium [13,14]. R_p^o was determined from the impedance spectrum of Al alloy 5083 (Al-Mg) after exposure in AS for 2 hours and found to be 44220 $ohm \cdot cm^2$. The time dependence of A_d was calculated using experimental values of the fit parameter R_p. Based on the time dependence of A_d for JJ5 in AS, the relationship between f_b and D was established. Using the same relationship, the time dependence of A_d was calculated for exposures at PH and KW. Similarly, the time dependence of D for JJ6 at the three locations was established. Impedance spectra for JJ1 and JJ2 did not follow the coating model [9-12] and R_p values could not be determined. Since visual rating data were not available, the time dependence of D could not be established. Instead, comparisons of the time dependence of experimental f_b values for JJ1 and JJ2 were performed.

The time dependence of D was found to follow the time law:

$$\log D = at + b \quad (1).$$

The time law in Eq. (1) can be replaced by:

$$\log D = a(t-t_o) \quad (2).$$

Linear regression analysis was applied to fit experimental log D - t curves to Eq. (1) and determine the parameters a and b for further statistical analysis. The t_o-values were then defined as $t_o = -(b/a)$, where t_o is the time at which log D = 1, i.e., the coating degradation area ratio is 1%.

Comparison of t_o-values was used to evaluate coating performance at different exposure sites and/or for different coating formulations with larger t_o-values indicating better coating performance. The Analysis of Variance (ANOVA) test [15,16] was performed on these t_o-

values in different ways, namely "inside solution", "between solution" and "interaction factors" to determine the statistical significance of observed differences in coating performance. The "inside solution" comparison was performed on t_o-values for each coating type at the same exposure site to reveal the effects of coating formulation on corrosion protection. The "between solution test" was performed on t_o -values of the same coating formulation for the three media to determine media effect on each coating type. The "interaction factors" comparison can discover interaction effects of coating formulation and media effects, i.e., whether there is a statistically significant difference in the performance of two different coating formulations exposed in two different media, i.e. NS vs. AS.

2.2.2. EN data. The time dependence of the potential of the two coupled samples (E_{coup}) and the coupling current (I_{coup}) has been discussed previously [1-3]. From the EN data the noise resistance $R_n = \sigma\{V(t)\}/\sigma\{I(t)\}$, defined as the ratio of the standard deviations of the potential noise ($\sigma\{V(t)\}$) and the current noise ($\sigma\{I(t)\}$) can be calculated. The spectral noise resistance $R^o_{sn} = \lim \{R_{sn}(f)\}$ for f --> 0, where $R_{sn}(f)$ is spectral noise and f is frequency, can be determined from power spectral density (PSD) plots for potential and current fluctuations [17,18] and can be used to evaluate coating degradation. Analysis of EIS and EN data obtained in the present project has shown that R_{sn} -plots were in general agreement with impedance modulus (log |Z|) Bode plots, provided suitable equipment was used to record EN data [20-22]. Therefore, analysis of EN measurements in the frequency domain provides the same information as Bode plots in the bandwidth Δf between 1 Hz to 1 mHz determined by the sampling rate $f_s = 2$ Hz (2 points/sec) and the sampling period T = 1024 seconds [1,3]. In those cases where no dc limit was observed in the spectral noise plots, R^o_{sn} values were calculated using the average of the last 10 data points. R_n values depend on Δf [19-21] and are related to the impedance of the system at $f = 0.5\ f_s$ [20,21]. Decreasing R_n and R^o_{sn} values are expected for a degrading coating system. The time dependence of R_n and R^o_{sn} has been presented previously [1-3]. Experimentally, poor agreement between spectral noise plots and impedance modulus plots was observed in the early stages of exposure and for very protective coating systems. These problems have been traced to insufficient sensitivity of the current noise measurement amplifier in the equipment used at PH and KW. The only experimental R^o_{sn} and R_n values that could be related to coating degradation were those for rapidly degrading coating systems for which the noise current signal was above the instrumentation limit. Therefore only limited use of EN data has been made in the analysis of coating degradation and the establishment of correlations between coating properties, exposure conditions and coating degradation.

3.0. EXPERIMENTAL RESULTS AND DISCUSSION

3.1. EIS/ESEM Results

Fig. 2a is a comparison between D-values for CR6 exposed in NS (PH and KW) and in AS calculated from f_b-values normalized using visual rating results determined after 110 days. The conversion factor for KW samples was assumed to be the same as that for PH samples. Very good agreement was found between visual rating data and D values (converted from f_b from EIS results) for the entire exposure period. The same procedure was applied to all other coating systems except for JJ1 and JJ2 for reasons explained previously. Experimental D-values were fit to Eq. (2) and calculated t_o-values were used to rank the relative performance of a given coating exposed to the different media or for different coatings in the same medium. D values for CR6 were the largest for AS and least for KW. After 222 days rust spots were documented for CR6 in AS (Fig. 2b) with a total

size similar to that given by the D value in Fig. 2a. Much smaller rust spots were observed in samples exposed at PH (Fig. 2c) in agreement with the results in Fig. 2a.

CR1. CR1 is an alkyd type coating system with alkyd high-solid as primer and low-VOC alkyd as midcoat and topcoat (Table I). Test panels exposed in AS and NS (PH) had very similar t_o-values and similar time dependence of D as shown in Fig. 3a indicating no significant differences in coating performance in these two media. For the test panels exposed in NS (KW) a different time dependence of D and a larger t_o-value were observed. The average t_o-value of about 300 days indicated that the delaminated (corroding) area for the CR1 coating system will reach 1% in less than one year exposure in a marine environment, making it one of the less protective coatings in this study. Blistering and rust spots were documented throughout the exposure period (Fig. 3b, c).

CR2. CR2 is an alkyd type coating system with the same primer as CR1, but with silicone alkyd as midcoat and topcoat. Rather low t_o-values were observed in the three media (Fig. 4a). CR2 reached D = 1 % in less than 300 days in all locations. The lowest value of t_o was observed in AS. For exposure in NS (KW), D remained very low for the first 100 days, but then increased sharply. Similar behavior was found for exposure in NS(PH) (Fig. 4a). For the final 5 months of exposure a similar time dependence was detected in the log D - $(t-t_o)$ plots shown in Fig. 4a. Corrosion damage, blistering and delamination were extensive on all panels after 200 days (Fig. 4b, c). Panels exposed in NS were colonized with bacteria and diatoms (Fig. 4d).

CR5. Significant differences in coating performance in different media were found for CR5 (Fig. 5a). For exposure in AS, D remained below 0.01% for the entire exposure time, while in NS, D increased continuously to values exceeding 0.2%. Based on the slopes of the curves in Fig. 5a and the t_o-values it can be concluded that KW was the most aggressive test site for the CR5 coating system. For samples exposed in NS (PH), degradation was not as severe as in KW, but D was expected to reach 1% in 642 days. The CR5 coating system performed much better in AS than in NS. The intact coating in AS was documented by ESEM after exposure for 200 days (Fig. 5b).

CR6. In plots of log D - $(t-t_0)$ very similar curves were observed at the three locations (Fig. 6) indicating that the rate of coating degradation was about the same. However, t_o-values indicated that the CR6 coating system degraded faster in AS than in NS. The NS (KW) medium seemed to attack CR6 less than the NS (PH) medium. These results suggested that the exposure medium had a different effect for the CR6 than for the CR5 coating system. The formulation for these two coatings differed only in the topcoat which was polyurethane for CR5 and latex for CR6.

CR7. For NS (PH and KW), the time dependence of D in the initial exposure period was very similar showing a sharp rise in the first three months followed by a plateau that lasted longer for AS than for NS (Fig. 7). In the final stages of exposure D started to increase again. Very similar t_o-values exceeding two years were estimated for exposure at PH and KW, although the particular time dependence of D in Fig. 7 made the extrapolation to D = 1% difficult.

JJ7. Coating system JJ7 is similar to CR7 except that it is an all-epoxy polyamide system, while CR7 has a latex topcoat (Table I). For exposure to AS and in NS (KW) similar coating degradation rates and t_o-values were observed indicating similar coating performance (Fig. 8a). For exposure in NS (PH) the rate of coating degradation was different and a higher t_o-value was found. Despite differences in degradation rates, after 200 days all samples were characterized by extensive rusting, blistering and delamination

(Fig. 8b, c, d). Corrosion products formed during exposure in NS (KW) were heavily entwined with helical bacterial filaments (Fig. 8 e).

JJ1 and JJ2. D-values for JJ1 and JJ2, which have a metallic zinc primer, could not be calculated since no visual rating data of rust spots were available. Therefore a qualitative comparison of coating damage was made based on experimental f_b-values. Very similar results were obtained for JJ1 in the three test media with initial high values increasing continuously with increasing exposure time (Fig. 9a). High f_b-values indicate that a large fraction of the metallic zinc primer was actively corroding providing cathodic protection to the steel substratum. Measurements with the scanning Kelvin probe detected a uniformly negative corrosion potential under the coating with values close to those for galvanized steel. Cathodic protection was verified by observation of the exposed samples with ESEM. Blisters were located on KW samples in association with microalgae (Fig. 9b, c). For JJ2 with an additional similar values as for JJ1 were determined for exposure at PH (Fig. 10a). Surface discolorations due to the presence of microalgae were found on samples exposed at PH after 400 days (Fig. 10b, c).

JJ3. Similar time dependence of coating delamination was observed at PH and KW for JJ3, which has a phosphate primer, indicating similar coating degradation rates at these two NS test sites (Fig. 11a). For exposure in AS degradation was less in the initial time period, but had reached similar D-values towards the end of exposure. After 200 days all surfaces showed rust spots (Fig. 11b, c, d). Corrosion products formed in NS were associated with large populations of bacteria (Fig. 11e, f).

JJ4. Results for JJ4 with an additional polyurethane topcoat compared to JJ3 shown in Fig. 12a indicate similar degradation rates. Based on t_o-values it can be concluded that delamination was less severe in AS than in NS (PH and KW). The significant increase of the t_o-values for JJ4 as compared to JJ3 at each location can be attributed to the protection provided by the topcoat. NS exposures were characterized by rusting (Fig. 12b) and the presence of bacteria within corrosion products (Fig. 12c).

JJ5. For JJ5 with IVD-Al primer very similar D-values were observed for the same reduced time $t-t_o$ and the t_o-values were about the same (Fig. 13a). For exposure in NS (PH), the JJ5 coating system degraded at a much faster rate and reached D = 1% much faster than for exposure in AS and NS (KW) even though less degradation was found in early exposure times. Samples exposed at KW had surface discoloration due to microalgae and some macrofouling after 300 days. No rust spots were observed (Fig. 13b, c). However, some rust spots were evident in PH exposures after 600 days (Fig. 13d).

JJ6. For JJ6 with the additional polyurethane topcoat (Table I), coating degradation occurred at a very slow rate (Fig. 14a). The time dependence of D was similar for exposure in AS and NS (KW). In NS (PH), D remained below 0.01% and increased in the last 100 days reaching values comparable to those found in AS and in NS (KW) (Fig. 14). Differences in time dependence of coating delamination observed for NS (PH and KW) compared to AS were the same for JJ5 (Fig. 13a) and JJ6 (Fig. 14a). A single large pit was detected after exposure at PH for 621 days (Fig. 14b).

Table II provides a summary of calculated t_o-values and standard deviations for the coating systems evaluated in this project. For CR9 no indication of coating damage was observed during the entire exposure period in any of the three test media.

3.2. ENA Results. Fig. 15 is a comparison of impedance spectra, spectral noise plots and R_n values obtained for CR2 after three exposure times. After exposure for one week

poor agreement between the impedance spectrum, the spectral noise plot and R_n was observed due to low current noise and instrumentation limitations. Since the noise current was below the instrumentation threshold, the current PSD plots were too high and R_n was too low (Fig. 15 a) [20,21]. As the coating degraded and the noise current increased, better agreement between the three sets of data was observed (Fig. 15 c). Good agreement between impedance spectra and spectral noise plots was obtained even for a very protective coating system such as CR9 with more sensitive instrumentation (Fig. 16). The instrument used in this measurement (ACM, U. K.) had better current measuring capability than that used at the remote test sites (Solartron model 1286 potentiostat). In general, it has been observed that R_{sn}-plots were identical with impedance spectra provided instrumental artifacts did not affect the measurement. The results in Fig. 15 and 16 illustrate the limited bandwidth Δf in which spectral noise plots can be obtained. R_n was fixed at f_s (Fig. 15). For a degraded coating system with a dc limit for $f < 1$ Hz, R^o_{sn} and R_n will be equal to R_p of the coating system, which is inversely proportional to A_d [9]. This allows determination of D from EN data. Similarly, D-values can be obtained using R_n and R_{sn}^o values normalized by visual rating data. The normalization procedure of EN data has been applied for CR6 and JJ3 samples exposed in AS and at PH.

The relationships between D and R_n or R_{sn}^o were established for AS and NS (PH), respectively, using the visual rating data obtained after about three months. Fairly good agreement between D-values obtained from R_n and R^o_{sn} values and visual rating results was found for CR6 in Fig. 17 and for JJ3 in Fig. 18, which also show the D-values based on f_b-values. Compared with results calculated from impedance measurements more scatter of the D-values from EN data was found, especially at early exposure times when difficulties with accurate measurements of current EN values were encountered. Better agreement between D-values calculated from EIS and EN data was found for longer exposure times when D exceeded 0.01% (Fig. 17 and 18).

3.3. Samples with intentional coating defects. Samples of the JJ series with intentional coating defects (Fig. 1) were exposed in NS (KW) and in AS for 30 days. EN data were collected at KW only for samples not cathodically protected, while in the AS laboratory tests EN data were obtained for cathodically protected and unprotected samples. E_{coup} values for JJ1 and JJ2 with a zinc plate primer were close to -1000 mV vs. Ag /AgCl (Fig. 19) similar to E_{corr} for zinc in seawater. The E_{coup}-values for all other JJ samples were about -700 mV which is close to E_{corr} for iron in seawater. While the zinc layer on steel in JJ1 and JJ2 provided cathodic protection to exposed steel in the defects, the same effect was not observed for JJ5 and JJ6 with an IVD-Al primer (Fig. 19a). Visual observation showed that the defects were covered with rust except for the JJ1 and JJ2 samples where calcareous deposits had formed (Fig. 19b-e).

The i_{coup}-values decreased with time for JJ1 and JJ2 (Fig. 20 a), while for the other samples i_{coup} remained at about the same level after 7 days immersion (Fig. 20 b, c). The time dependence of R^o_{sn}-values for the JJ samples with defects is shown in Fig. 21. For JJ3 and JJ4, R^o_{sn} decreased with exposure time, while for JJ1 and JJ2, R^o_{sn} increased. No significant changes were found for the other samples (Fig. 21). In Fig. 21a the R^o_{sn}-values for JJ1 and JJ2 were almost the same with an increasing tendency with exposure time. The product $R^o_{sn} \times i_{coup}$ had the same approximate value of 10 mV for all coating systems (Fig. 22). This result is similar to the well-known relationship between the corrosion current I_{corr} and R_p ($I_{corr} \times R_p = B$). The parameter B defined as $B = (b_a \cdot b_c)/(2.3(b_a+b_c))$, where b_a and b_c are the anodic and cathodic Tafel slopes, respectively, equals 10.4 mV for

b_a = 120 mV and b_c = 30 mV. B = 10 mV is very similar to the product of R^o_{sn} x i_{coup} from noise measurements (Fig. 22). In principle, I_{coup} does not equal I_{corr} and R^o_{sn} equals R_p only for spectral noise plots which are independent of frequency [7,8,20]. Nevertheless, the results in Fig. 22 suggest that the mechanism of the corrosion reaction occurring in the intentional coating defects is very similar for all coating formulations.

For JJ series samples with intentional defects coupled to galvanized steel, R_n and R^o_{sn} data were obtained during immersion in AS for 30 days. (Fig. 23). E_{coup} for all coupled samples was about -1000 mV Vs Ag/AgCl. R_n and R^o_{sn} increased with time for all samples. These increases were most likely due to formation of calcareous deposits in defects which increased the pore resistance R_{po}. Impedance spectra obtained during immersion in AS confirmed the assumption that R_{po} increased as defects filled with calcareous deposits. As shown in Fig. 24 the spectra changed from a one-time-constant mechanism at early exposure times to spectra containing the polymer coating capacitance C_c at the highest frequencies and R_{po} at the lower frequencies where the EN data were recorded. R_n and R^o_{sn} are therefore related to R_{po}. Results shown in Fig. 23 demonstrate that it is possible to follow changes in properties of the coating defects with ENA.

3.4. Samples exposed to mixed communities of bacteria.

All samples of the CR and the JJ series were exposed to three types of mixed communities of bacteria and a control medium for different time periods. Samples of the JJ series with intentional defects connected to zinc anodes were exposed to the same solutions for 30 days.

3.4.1. CR series and JJ series samples.

JJ coatings performed better than CR coatings in laboratory exposures to three mixed communities of marine bacteria. Roughly half the CR- coated panels showed signs of localized corrosion associated with large numbers of bacterial cells. All CR2 panels showed signs of blistering after 6 months, indicating that the zinc primer and silicone alkyd mid- and topcoats provided little protection under the exposure conditions. Only the JJ-2 panels showed signs of corrosion after 10 months. Large numbers of bacterial cells were associated with all corrosion products.

EIS results for the CR and JJ series samples exposed to three mixed communities of marine bacteria and a control solution have been discussed in previous reports [1-3].

3.4.2. JJ Series samples with intentional defects. JJ coupons containing intentional defects (Fig. 1) connected to zinc anodes were exposed to three mixed communities of marine bacteria (P14, 49Z and CG59) known to contain SRB in anaerobic media [1-3]. The chemistry and microbial colonization of the defects varied among different coatings exposed to the same microbial consortium and within a single coating exposed to different microorganisms. Unlike the NS exposures, no calcareous deposits were detected within the intentional defects. In most cases defects in control samples (uninoculated) were filled with zinc or iron phosphates, while the defects in samples that had been inoculated had been derivitized to varying extents by sulfides. The source of the zinc was the dissolving anode and the source of the phosphate was the culture medium. Blistering was observed in areas proximate and remote to the intentional defects in JJ3 and JJ4 controls (uninoculated) (Fig. 25a, b) . Both JJ3 and JJ4 coatings showed some flaking around defects after exposure to bacteria for 70 days (Fig. 26a, b). In exposure to NS bacteria were concentrated within defects and were consistently co-located with iron oxide

corrosion products. SRB used in the laboratory experiments represent only a small subsample of the total natural population found in the marine environment. In anaerobic media only one defect had an accumulation of iron oxides (coating JJ6 exposed to culture 49Z) (Fig. 27a). In that case numerous bacteria were co-located with the oxide corrosion products (Fig. 27b). Sulfide corrosion products in all defects were not necessarily accompanied by large concentrations of cells. Instead, SRB growing in the medium produced sulfides that behaved like waterborne sulfides.

3.5. Statistical Analysis of EIS Data.

The time dependence of the delaminated area ratio D for each coating system exposed at the three locations followed Eq. 1 and 2. The fit parameters a and t_o listed in Table III were determined through a linear regression fitting process. The t_o-value is the time elapsed for each coating system to reach D = 1 %.

Significance tests were performed on the regression equations based on Eq. 2 by calculating the statistical F-values. Significant differences in D-values occur if F exceeds the critical value F_{crit}. The confidence level was defined here at 99%. The significance test was first performed on the slope a of the regression lines. It was not necessary to perform the significance test on t_o if the slope was determined as significantly different. The statistical F-values were calculated for the intercepts of two regression lines only if the slopes were statistically identical. The coating damage functions have been tested first for the significance of time dependence, i. e. for the significance of the difference between the slopes of these damage function and a slope of zero. The results showed that all damage functions were significantly dependent on time. The comparison for the coating damage functions was performed in two categories: "between solution" and "inside solution". The "between solution" comparison compared a certain coating system in the three different media to reveal the effects of the exposure medium on the rate of coating degradation. The "inside solution" comparison compared different coating formulations in the same medium to discover the effects of coating formulation on corrosion protection of steel.

3.5.1. "Between Solution" Comparisons. Table IV and Fig. 3 show that CR1 performed significantly different in the three different media. The damage function for CR1 exposed at KW had the largest slope indicating that CR1 deteriorated at the fastest rate at KW once the polymer coating had started to degrade (Table III). However, the t_o-value suggests that CR1 exposed at KW reached D = 1% at a much longer time than at PH and in AS. Apparently CR1 started to degrade first in AS, but had the slowest degradation rate.

Significantly different coating degradation rates were observed for CR2 during exposure in AS and NS (Table IV, Fig. 4). The slopes of the damage functions were not statistically different for exposure in PH and KW (Table IV), however a significant difference was observed for the t_o-values.

The most significant difference of coating degradation rates for the CR5 coating system was found in a comparison of the slopes of the damage functions for exposure in AS and at KW (Table IV, Fig. 5). A significant difference of t_o-values was found for CR5 exposed in AS and PH. Based on the results in Tables III and IV it may be concluded that NS causes more severe attack for the CR5 coating system than AS.

Table IV and Fig. 6 indicate no significant differences in the slopes of the damage functions for CR6, while a comparison of the t_o-values suggests significant differences in the extent of coating degradation at any given exposure time. The results in Table III indicate that for

CR6 AS was the most aggressive medium, while NS at KW seemed to be less corrosive towards the polymer coating than NS at PH.

The results of the statistical analysis for CR7 were very similar to those for CR6 since no significant differences were observed for the slopes of the damage functions, but significant differences were indicated for the t_o-values (Table IV, Fig. 7). Based on the t_o-values it can be concluded that CR7 degraded faster in NS (PH and KW) than in AS.

Since visual rating data were not available for JJ1 and JJ2 the rate of coating degradation was determined qualitatively based on the time dependence of f_b, which was expressed as $\log f_b = a_1 t + b_1$. Based on the experimental data in Fig. 9, the fit parameters in Table IIIc and the results of the statistical analysis in Table IV it can be concluded that coating degradation of JJ1 occurred at about the same rate in all three exposure media. For JJ2 NS at PH was the most aggressive medium, while degradation occurred at similar rates at KW and in AS (Table IV, Fig. 10).

Table IV and Fig. 11 suggest that the two NS media statistically had the same effects on the JJ3 coating systems. The slope comparison in Table IV demonstrates significant differences between AS and NS. The slope and t_o-values from Table III indicate that JJ3 started to degrade earlier and with a faster rate in AS than in NS.

The slope comparison for JJ4 (Fig. 12 and Table IV) suggests that the coating degradation rate for JJ4 was independent of exposure medium. JJ4 performed statistically the same in AS and in PH media. The t_o-values (Table III) indicated that the JJ4 coating system was attacked more severely at KW.

The slope and t_o-values from Table III and Fig. 13 suggest that JJ5 degraded the least in AS. NS attacked the JJ5 coating system more severely than AS. The coating performance can be ranked as AS > KW > PH.

The damage functions for JJ6 were significantly different in terms of their time dependence (Table IV, Fig. 14). The effect of the exposure medium was significantly different in terms of coating degradation rate. The slope comparison suggested that the ranking for JJ6 in terms of coating performance was AS > KW > PH, which is consistent with the results from t_o-values.

3.5.2. "Inside Solution" Comparison.

CR1 vs. CR2. Comparison of the performance of CR1 and CR2 reveals the effects of the alkyd coating as midcoat and topcoat on coating performance at the three different locations. Table Va shows that CR1 and CR2 provided the same degree of corrosion protection in AS, but performed differently in exposure at PH and KW. The low-VOC alkyd and silicone alkyd midcoat showed insignificant differences in performance in AS media. However, the two alkyd coatings performed significantly different in NS. The t_o-values (Table III) suggest that CR1 does not provide longer lasting protection in NS than CR2 indicating that the silicone alkyd midcoat provided better corrosion protection in NS.

CR5 vs. CR6. Comparison of the D-values for CR5 and CR6 should indicate possible differences between corrosion protection provided by polyurethane and latex as topcoats. Corrosion protection of steel provided by CR6 and CR5 was significantly different in AS and PH media, but statistically the same in KW (Table IVb). The t_o-values (Table III) suggest that the polyurethane topcoat provided better protection than latex in AS and in NS

at PH. However, the insignificant differences between the damage functions for CR5 and CR6 at KW suggest that polyurethane and latex topcoats performed similarly at KW.

CR6 vs. CR7. Comparison of the results for CR6 and CR7 allows one to evaluate the effects of primer composition on corrosion resistance. According to the results in Table Vc, CR7 and CR6 performed significantly different in the three media. The t_o-values (Table III) suggest that CR7 was a more protective coating than CR6 at the three locations. Apparently the polyamide primer provided better corrosion protection than the Zn-rich primer in marine environments.

JJ3 vs. JJ4. The additional polyurethane topcoat in the JJ4 coating provided improved corrosion protection for the steel with a phosphate primer in the three media (Tables Table III and Vd).

JJ5 vs. JJ6. The comparison of the results for JJ5 and JJ6 reveals the effects of the additional polyurethane topcoat for mild steel with the IVD-Al primer. JJ5 and JJ6 performed significantly different in AS and PH, but had statistically the same D-values at KW (Table Ve). The t_o- and slope values (Table III) suggested that JJ6 was a better coating system in AS and PH media than JJ5. However, JJ5 and JJ6 showed insignificant differences in KW media indicating that the polyurethane topcoat did not provide additional corrosion protection at KW.

JJ7 vs. CR9. CR9 did not show any indications of coating degradation during the entire exposure period in NS and AS, while JJ7 degraded very rapidly and reached D = 1% in less than one year (Table III). CR9 was processed based on specifications for type I epoxy polyamide paint, while JJ7 was processed in California as a type III coating. As shown in Table I the coating system on JJ7 was significantly thinner than that on CR9.

4.0. SUMMARY AND CONCLUSIONS

The newly developed approach for collection of experimental impedance and noise data from remote marine test sites has produced data of excellent quality. Damage functions have been determined based on impedance data that are in agreement with those based on visual observation on the polymer coated steel panels for periods exceeding one year. Less satisfactory results were obtained from analysis of EN data due to instrumental artifacts. Its has been demonstrated that spectral noise plots which are derived from PSD plots agree with impedance spectra provided that instrumentation with sufficient resolution of the current noise measurement is employed.

Statistical analysis of the damage functions for the CR series has indicated differences in performance for coatings with different primers, midcoats or topcoats exposed to NS and AS. The polyurethane topcoat provided longer lasting protection for the JJ series in AS than in NS pointing to attack by bacteria.

The affinity of marine bacteria for iron corrosion products has been documented in experiments with samples containing intentional defects. Very few bacteria were observed on coated steel samples with a metallic zinc primer with a potential of about - 1 V vs. Ag/AgCl, while defects in coated samples with a phosphate primer with a potential of about -0.7 V were heavily colonized. Cathodic protection prevented rusting and sharply reduced the number of bacteria in defects. Spatial relationships between bacteria and corrosion products can not be simply interpreted as causal, i.e., that bacteria were in all cases responsible for corrosion when they were co-located with concentrations of corrosion products. In previous experiments reported in the literature large concentrations of bacteria

were always co-located with corrosion products. The temptation has been to interpret the spatial relationship as causal, i.e., that corrosion was in fact due to the presence and activities of the bacteria. Bacteria preferentially colonize scratches, pinholes and holidays in coatings. These same areas have been the first to exhibit localized corrosion in abiotic artificial seawater. The present study has demonstrated that bacteria are preferentially attracted to iron corrosion products in coating defects. The nature of that attraction cannot be determined by this study.

ACKNOWLEDGMENT

The support and encouragement of Dr. A. J. Sedriks of the Naval Research Office under Contract No. N00014-94-1-0026 is greatly appreciated. The authors acknowledge the help of D. Polly at NCEL, Port Hueneme, CA and K. Lucas and R. Foster at NRL, Key West, FL in setting up and maintaining the CEEL/USC equipment at their respective test sites.

5.0. REFERENCES

1. F.Mansfeld, H. Xiao, L. T. Han, C. C. Lee, J. Jones-Meehan and B. J. Little, " The Impact of Microbiologically Influenced Corrosion on Protective Polymer Coatings", Annual Report No. 1, Contract No. 00014-94-1-0026, December 1994.

2. F. Mansfeld, H. Xiao, L. T. Han, C. C. Lee, J. Jones-Meehan and B. J. Little, " The Impact of Microbiologically Influenced Corrosion on Protective Polymer Coatings", Annual Report No. 2, Contract No. 00014-94-1-0026, December 1995.

3. F. Mansfeld, L. T. Han, C. C. Lee, G. Zhang, J. Jones-Meehan, and B. J. Little, " The Impact of Microbiologically Influenced Corrosion on Protective Polymer Coatings", Annual Report No. 3, Contract No. 00014-94-1-0026, June 1996.

4. H. Xiao, "Development of the Electrochemical Noise Technique and its Application to Evaluation of Localized Corrosion Phenomena", Ph. D. Thesis, University of Southern California, Sept. 1995.

5. F. Mansfeld, H. Xiao, C. C. Lee, and L. T. Han, "Evaluation of Coating Performance with Electrochemical Impedance Spectroscopy and Electrochemical Noise Analysis", Corrosion/95, paper No. 530, NACE.

6. L. T. Han, "Evaluation of Methods of Corrosion Protection Using Electrochemical Techniques", Ph. D. Thesis, University of Southern California, November, 1996.

7. H. Xiao, L. T. Han, C. C. Lee and F. Mansfeld, Corrosion, 53, 412 (1997).

8. F. Mansfeld, L. T. Han, C. C. Lee and G. Zhang, " Electrochemical Impedance and Noise Data for Polymer Coated Steel Exposed at Remote Marine Test Sites ", Proc. Tri-Service Conference on Corrosion, 1997.

9. F. Mansfeld, J. Appl. Electrochem. 25, 187 (1995).

10. S. Haruyama, M. Asari and T. Tsuru, in " Corrosion Protection by Organic Coatings", Electrochem. Soc., Proc. Vol. 87-2, 197 (1987).

11. C. H. Tsai, Ph. D. thesis, University of Southern California, Aug. 1992.

12. F. Mansfeld and C. H. Tsai, Corrosion 47, 958 (1991).

13. R. D. Armstrong, J. D. Wright and T. M. Handyside, J. Appl. Electrochem. 22 795 (1992).

14. R. D. Armstrong and J. D. Wright, Corrosion Science 33, 1529 (1992).

15. G. E. P. Box, W. G. Hunter and J. S Hunter, " Statistics for Experimenters", Wiley & Sons, Inc., New York, 1978

16. E. K. Bowen and M. K. Starr, " Basic Statistics for Business and Economics ", McGraw-Hill Inc., New York, 1982

17. H. Xiao and F. Mansfeld, J. Electrochem. Soc. 141, 2332 (1994)

18. F. Mansfeld and H. Xiao, ASTM STP 1277, 59 (1996).

19. U. Bertocci and F. Huet, Corrosion 51, 131 (1995).

20. F. Mansfeld and C. C. Lee, J. Electrochem. Soc. 144, 2068 (1997)

21. F. Mansfeld, L. T. Han and C. C. Lee, J. Electrochem. Soc. 143, L286 (1996).

22. F. Huet, J. Electrochem. Soc. 142. 2861 (1995).

23. C. Chen and F. Mansfeld, Corr. Sci. 39, 409 (1997)

24. L. T. Han and F. Mansfeld, Corr. Sci. 39, 199 (1997)

25. F. Mansfeld, C. Chen, C. C. Lee and H. Xiao, Corr. Sci. 38, 497 (1996)

Table I. Composition of Coating Systems

a. CR-series :

Sample Name	CR1	CR2	CR5	CR6	CR7	CR9
Substrate	Hot Rolled Steel	Hot Rolled Steel	Hot Rolled Steel	Hot Rolled Steel	Hot Rolled Steel	Hot Rolled Steel
Primer	Alkyd high solid[1]	Alkyd high solid[1]	Zn-rich Primer[4]	Zn-rich Primer[4]	Epoxy Polyamide[5]	Epoxy Polyamide[5]
Midcoat	Low VOC Alkyd[2]	Silicone Alkyd[3]	Epoxy Polyamide[5]	Epoxy Polyamide[5]	Epoxy Polyamide[8]	Epoxy Polyamide[8]
Topcoat	Low VOC Alkyd[2]	Silicone Alkyd[3]	Urethane[6]	Latex[7]	Latex[7]	Epoxy Polyamide[9]

b. JJ-series :

Sample Name	JJ1	JJ2	JJ3	JJ4	JJ5	JJ6	JJ7
Substrate	Cold RolledSteel	Cold RolledSteel	Cold RolledSteel	Cold RolledSteel	Cold RolledSteel	Cold RolledSteel	Cold RolledSteel
Primer	Zinc plate[a]	Zinc plate[a]	Phosphate coat[d]	Phosphate coat[d]	IVD-Al[e]	IVD-Al[e]	Epoxy Polyamide[f]
Midcoat	Epoxy[b]	Epoxy[b]	Epoxy[b]	Epoxy[b]	Epoxy[b]	Epoxy[b]	Epoxy Polyamide[g]
Topcoat		Polyurethane[c]		Polyurethane[c]		Polyurethane[c]	Epoxy Polyamide[h]

NOTE:
1. TT-P-645B.
2. TT-E-489H.
3. TT-E-49.
4. SSPC-20, type 2.
5. MIL-P-24441,Formula 150.
6. MIL-C-85285.
7. MIL-P-28578.
8. MIL-P-24441,Formula 151.
9. MIL-P-24441,Formula 152.

a. Zinc plate per QQ-Z-325 Rev. C (Type II , Class 2).
b. 2 coats of epoxy polyamide primer MIL-P-23377 Rev. F (Type I class C) per MIL-F-18264 REV.D AMD.I.
c. 1 coat of MIL-C-85285 REV.B (AS) AMD.2 polyurethane per MIL-F-18264 REV.D AMD.1 color #36375 lusterless gray of FED-STD-595.
d. Phosphate coat DOD-P-16232 REV.F (Type Z class 3) ; hydrogen embrittlement relieved for 8 hours at 210-225 degree.
e. IVD aluminum per MIL-C-83488-C (Notice 1. Type II Class I)
f. MIL-P-24441/20, Rev. B Formula 150, type III
g. MIL-P-24441/21, Rev. B Formula 151, type III
h. MIL-P-24441/22, Rev. B Formula 152, type III

Table II : t_o values (days); and standard deviations (SE)

	AS		PH		KW	
coatying type	t_o	SE	t_o	SE	t_o	SE
CR1	256.84	26.41	259.21	20.53	337.82	29.35
CR2	187.07	28.29	206.82	23.42	288.66	24.44
CR5	882.46	147.69	642.37	64.19	404.41	24.33
CR6	274.27	20.15	352.12	9.72	490.75	48.15
CR7	894.13	102.17	715.7	68.67	723.2	57.8
CR9	n.d.		n.d.		n.d.	
JJ3	323.77	31.721	367.27	47.58	407.24	22.29
JJ4	752.84	9.66	641.3	72.39	572.28	24.09
JJ5	942.06	91.58	463.95	33.11	932.39	104.8
JJ6	2185.1	295.9	890.76	186.6	1140.6	223.03
JJ7	278.97	41.9	391.81	23.99	297.53	18.88

note : n.d : no damage

Table III (a). Damage functions : $y = a(t-t_o)$, where y=lnD (%)

	AS		PH		KW	
Coating	slope : a	t_o (day)	slope : a	t_o (day)	slope : a	t_o (day)
CR1	0.0158	256	0.0198	259	0.0256	337
CR2	0.0188	187	0.039	206	0.0307	288
CR5	0.00773	882	0.00913	642	0.0151	404
CR6	0.0176	274	0.0159	352	0.0144	491
CR7	0.0091	894	0.0069	715	0.0089	723
JJ3	0.0228	324	0.0167	367	0.0144	407
JJ4	0.0079	753	0.0089	641	0.0092	572
JJ5	0.0042	942	0.0162	464	0.0036	932
JJ6	0.00126	2185	0.0063	891	0.0022	1140
JJ7	0.0272	279	0.0179	392	0.034	298

Table III (b) : Damage functions : $y = at + b$, where $y=\log f_b$ (Hz),

	AS		PH		KW	
Coating	slope : a	b (Hz)	slope : a	b (Hz)	slope : a	b (Hz)
JJ1	0.0078	1.9	0.0095	1.7	0.0063	1.9
JJ2	0.0038	1.4	0.0062	2.4	0.004	1.4

Table IV. Between solution comparison :

	Slope comparisons				t_o comparisons		
Coating type	Comparing pairs	F	F_{crit}	Significance	F	F_{crit}	Significance
CR1	AS-PH	8.84	7.31	yes	n.c.		
	AS-KW	23.61	7.31	yes	n.c.		
	PH-KW	9.24	7.31	yes	n.c.		
CR2	AS-PH	44.15	7.56	yes	n.c.		
	AS-KW	37.57	7.08	yes	n.c.		
	PH-KW	2.015	7.56	no	17.35	7.08	yes
CR5	AS-PH	1.09	7.31	no	101	7.31	yes
	AS-KW	34.09	7.08	yes	n.c.		
	PH-KW	48.1	7.08	yes	n.c.		
CR6	AS-PH	4.14	7.31	no	2073	7.31	yes
	AS-KW	4.9	7.31	no	5692	7.31	yes
	PH-KW	1.452	7.31	no	10.56	7.31	yes
CR7	AS-PH	0.02	7.31	no	108	7.31	yes
	AS-KW	5.89	7.31	no	83	7.31	yes
	PH-KW	5.783	7.31	no	302	7.31	yes
JJ3	AS-PH	16.62	7.31	yes	n.c		
	AS-KW	43.34	7.08	yes	n.c.		
	PH-KW	2.81	7.08	no	2.13	7.31	no
JJ4	AS-PH	0.63	7	no	5.37	7.08	no
	AS-KW	6.44	6.85	no	155.5	7	yes
	PH-KW	0.093	6.85	no	29.23	7	yes
JJ5	AS-PH	263	7.08	yes	n.c.		
	AS-KW	0.96	7	no	299.2	7.08	yes
	PH-KW	287.8	7	yes	n.c.		
JJ6	AS-PH	76.26	7.08	yes	n.c.		
	AS-KW	13.64	6.7	yes	n.c.		
	PH-KW	25.03	6.7	yes	n.c.		
JJ7	AS-PH	12.6	7.08	yes	n.c.		
	AS-KW	17.92	7.31	yes	n.c.		
	PH-KW	120.1	7.31	yes	n.c		
JJ1	AS-PH	1.99	7.08	no	4.86	7.08	no
	AS-KW	2.62	7.08	no	9.93	7.08	yes
	PH-KW	9.9	7.08	yes	n.c.		
JJ2	AS-PH	12.04	6.7	yes	n.c.		
	AS-KW	0.84	6.7	no	0.84	6.7	no
	PH-KW	6.09	6.7	no	692	6.7	yes

note : n.c.: no need to compare

Table V. Inside solution comparison :

(a) CR1 vs CR2

	Slope comparison			t_o comparison		
location	F	F_{crit}	Significance	F	F_{crit}	Significance
AS	2.42	7.43	**no**	1.99	7.86	**no**
PH	111	7.31	**yes**	n.c.		
KW	41.01	7.08	**yes**	n.c.		

(b) CR5 vs CR6

	Slope comparison			t_o comparison		
location	F	F_{crit}	Significance	F	F_{crit}	Significance
AS	43.4	7.31	**yes**	n.c.		
PH	48.5	7.19	**yes**	n.c.		
KW	0.409	7.08	**no**	1.44	7.08	**no**

(c) CR6 vs CR7

	Slope comparison			t_o comparison		
location	F	F_{crit}	Significance	F	F_{crit}	Significance
AS	64.25	7.31	**yes**	n.c.		
PH	163.15	7.19	**yes**	n.c.		
KW	27.07	7.08	**yes**	n.c.		

(d) JJ3 vs JJ4

	Slope comparison			t_o comparison		
location	F	F_{crit}	Significance	F	F_{crit}	Significance
AS	48.8	6.9	**yes**	n.c.		
PH	16.2	7.19	**yes**	n.c.		
KW	56.41	6.85	**yes**	n.c.		

(e) JJ5 vs JJ6

	Slope comparison			t_o comparison		
location	F	F_{crit}	Significance	F	F_{crit}	Significance
AS	108	6.85	**yes**	n.c.		
PH	103	7.19	**yes**	n.c.		
KW	0.74	6.9	**no**	4.46	7.08	**no**

(f) JJ1 vs JJ2

	Slope comparison			intercept comparison		
location	F	Fcrit	Significance	F	Fcrit	Significance
AS	95.64	7.01	**yes**	n.c.		
PH	8.73	7.01	**yes**	n.c.		
KW	9.89	7.01	**yes**	n.c.		

Note : n.c. no need to compare

Appendix A

Tables A1 - A3 give a summary of the exposure program used in this project. Each Table lists the six coatings in the CR series and the seven coatings in the JJ series. For samples of the CR series the average coating thickness of each side of the sample is given, while for the JJ series only the average thickness of the coating was provided by the vendor (AAA Plating, Compton, CA). A large difference in coating thickness was noted for CR9 prepared by the Steel Structures Painting Council (SSPC), Pittsburgh, PA and JJ7 prepared by AAA Plating.

The dates at which the samples were first exposed are listed in Table A1 - A3. Exposure was initiated in July 1994 at PH (Table A1) and in the laboratory (Table A3), while tests were started at KW in May 1995 (Table A2). Since the equipment for recording of electrochemical data had to be moved from PH to KW in May 1995, such data were only collected once a month at PH using the equipment for laboratory studies at CEEL/USC starting in March 1995.

The dates at which samples were removed are also listed in Tables A1 - A3 together with the final visual rating of each sample at PH (Table A1) and in the laboratory taken at the time of removal (Table A3). In some cases only one sample of the exposed pair was removed since the coating on the other sample was considered intact based on visual observation. In this case impedance data were collected for the remaining sample using a 3-E approach. No visual rating data are listed for JJ1 and JJ2 samples with a metallic zinc primer.

The potential of the coupled electrodes E^{i}_{coup} recorded within the first two days of exposure is also listed in Tables A1 - A3. E^{f}_{coup} is the potential recorded at the removal date of one or both samples of a particular coating system. Very negative E^{i}_{coup} values were recorded for JJ1, JJ2, JJ5 and JJ6 samples with metallic zinc or IVD Al primers, respectively. Similar values were recorded for CR5 with a zinc-rich primer and a polyurethane topcoat, but not for CR6, which had the same primer, but a latex topcoat (Table I).

Table A.1. Exposure Data for Port Hueneme (PH)

Sample	Coating thickness (μm)	immersed	removed	exposure	VR	E_{coup}^{I}	E_{coup}^{T}
CR1		date	date	(days)			
A30	154/168	7/28/94	5/2/95	278	8.5	-562	-649
A32	144/173	7/28/94	10/19/96	811	9		
CR2							
B26	121/131	7/28/94	2/21/95	208	6.5	-99	-552
B33	118/127	7/28/94	2/21/95	208	7		
CR5							
C25	307/279	7/28/94	11/30/95	490	8.5	-907	-719
C33	302/297	7/28/94	11/30/95	490	8.5		
CR6							
D32	274/290	7/28/94	2/22/95	209	7.5	-439	-535
D33	287/295	7/28/94	2/22/95	209	7.5		
CR7							
E25	187/204	7/28/94	5/2/95	278	8	-93	-211
E31	189/191	7/28/94	10/19/96	811	7.5		
CR9							
F26	180/196	7/28/94	10/19/96	811	9.5	-383	-56
F28	179/197	7/28/94	10/19/96	811	9.5		
JJ1							
1AS	53*	7/28/94	9/6/95	405		-1006	-1094
2AS	53*	7/28/94	11/30/95	490			
JJ2							
3AS	83*	7/28/94	9/6/95	405		-1112	-980
4AS	83*	7/28/94	9/6/95	405			
JJ3							
5AS	43*	7/28/94	2/22/95	209	8.5	-453	-577
6AS	43*	7/28/94	2/22/95	209	7.5		
JJ4							
7AS	76*	7/28/94	9/6/95	405	6	-150	-628
8AS	76*	7/28/94	9/6/95	405	6		
JJ5							
9AS	81*	7/28/94	4/9/96	621		-993	-687
10AS	81*	7/28/94	10/19/96	811			
JJ6							
11AS	81*	7/28/94	4/9/96	621		-929	-723
12AS	81*	7/28/94	10/19/96	811			
JJ7							
13AS	81*	7/28/94	5/1/95	270	8	-647	-540
14AS	81*	7/28/94	11/30/95	483	8		

Note : * : average values for all samples

VR : Visual Rating number

E_{coup} was measured in mV vs Ag/ AgCl

Table A.2. Exposure Data for Key West (KW)

Sample	Coating thickness (μm)	immersed	removed	exposure	E_{coup}^{I}	E_{coup}^{I}
CR1		date	date	(days)		
A25	159/180	5/19/95	4/19/96	336	-608	-502
A28	139/160	5/19/95	9/25/97	796		
CR2						
B27	135/135	5/19/95	4/19/96	336	-634	-484
B34	221/246	5/19/95	4/19/96	336		
CR5						
C27	221/246	5/19/95	4/19/96	336	-1000	-449
C29	279/218	5/19/95	9/25/97	796		
CR6						
D30	254/221	5/19/95	4/19/96	336	-680	-473
D34	239/234	5/19/95	4/19/96	336		
CR7						
E26	193/178	5/19/95	4/19/96	336	-605	-478
E34	178/186	5/19/95	9/25/97	796		
CR9						
F30	196/205	5/19/95	9/25/97	796	0	-28
F32	200/189	5/19/95	9/25/97	796		
JJ1						
1KW	53*	5/19/95	4/19/96	336	-1034	-947
2KW	53*	5/19/95	9/25/97	336		
JJ2						
3KW	83*	5/19/95	9/25/97	796	-966	-963
4KW	83*	5/19/95	9/25/97	796		
JJ3						
5KW	43*	5/19/95	4/19/96	336	-202	-550
6KW	43*	5/19/95	4/19/96	336		
JJ4						
7KW	76*	5/19/95	9/25/97	796	-124	-607
8KW	76*	5/19/95	9/25/97	796		
JJ5						
9KW	81*	5/19/95	4/19/96	336	-915	-652
10KW	81*	5/19/95	9/25/97	796		
JJ6						
11KW	81*	5/19/95	9/25/97	796	-892	-634
12KW	81*	5/19/95	9/25/97	796		
JJ7						
13KW	81*	5/19/95	4/19/96	336	-543	-495
14KW	81*	5/19/95	9/25/97	796		

Note : * : average values for all samples

VR : Visual Rating number

E_{coup} was measured in mV vs Ag/ AgCl

Table A.3. Exposure Data for Artificial Seawater (AS)

Sample	Coating thickness (μm)	immersed date	removed date	exposure (days)	VR	E_{coup}^{i}	E_{coup}^{f}
CR1							
A29	165/157	7/18/94	7/20/97	1096	9	-633	-529
A34	172/159	7/18/94	2/28/95	225	6.5		
CR2							
B28	140/117	7/18/94	9/6/95	415	6	-602	-476
B30	124/118	7/18/94	2/28/95	225	3.5		
CR5							
C28	264/236	7/21/94	7/20/97	1097	9	-991	-451
C31	264/254	7/21/94	2/28/95	222	8.5		
CR6							
D27	213/226	7/21/94	7/20/97	222	6.5	-565	-481
D28	216/234	7/21/94	4/12/96	222	6.5		
CR7							
E28	186/205	7/21/94	7/20/97	1097	6	-44	-408
E29	197/205	7/21/94	7/20/97	634	7		
CR9							
F25	181/191	7/18/94	5/4/95	1097	9.5	-81	-47
F33	181/187	7/18/94	5/4/95	1097	9.5		
JJ1							
1AS	53*	7/21/94	5/4/95	287		-1114	-906
2AS	53*	7/21/94	5/4/95	287			
JJ2							
3AS	83*	7/18/94	7/20/97	1097		-1116	-910
4AS	83*	7/18/94	7/20/97	1097			
JJ3							
5AS	43*	7/18/94	4/12/96	637	7	-295	-505
6AS	43*	7/18/94	4/12/96	637	8		
JJ4							
7AS	76*	7/21/94	6/7/96	690	7	-183	-560
8AS	76*	7/21/94	6/7/96	690	7.5		
JJ5							
9AS	81*	7/21/94	4/12/96	634		-728	-959
10AS	81*	7/21/94	4/12/96	634			
JJ6							
11AS	81*	7/21/94	7/20/97	1097		-901	-715
12AS	81*	7/21/94	7/20/97	1097			
JJ7							
13AS	81*	7/18/94	2/28/95	225	6.5	-575	-458
14AS	81*	7/18/94	5/4/95	290	7		

Note : * : average values for all samples

VR : Visual Rating number

E_{coup} was measured in mV vs Ag/ AgCl

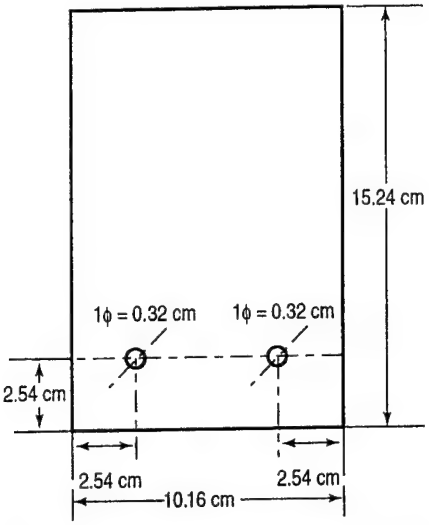

Fig. 1. Schematic diagram for samples with artificial defects in polymer coating.

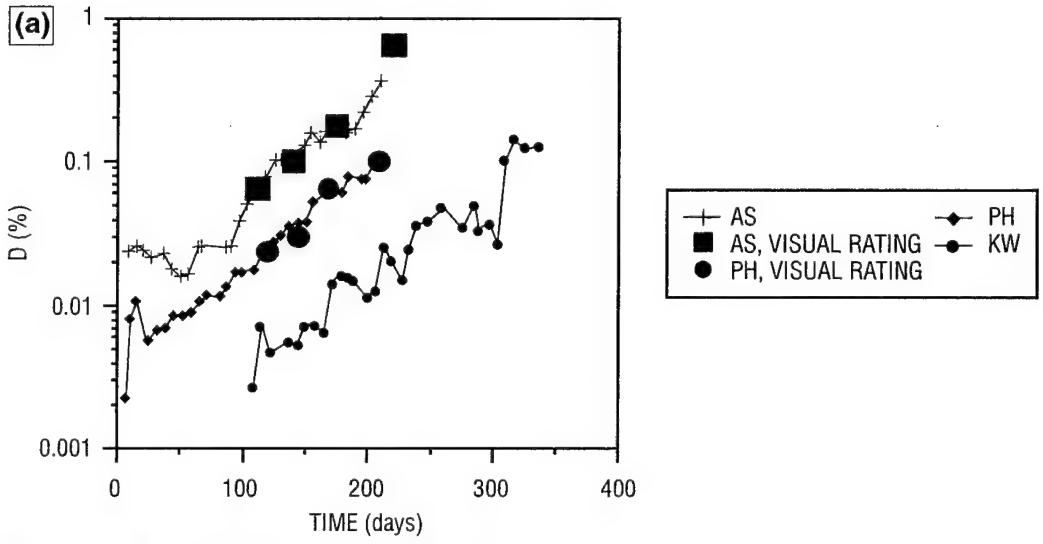

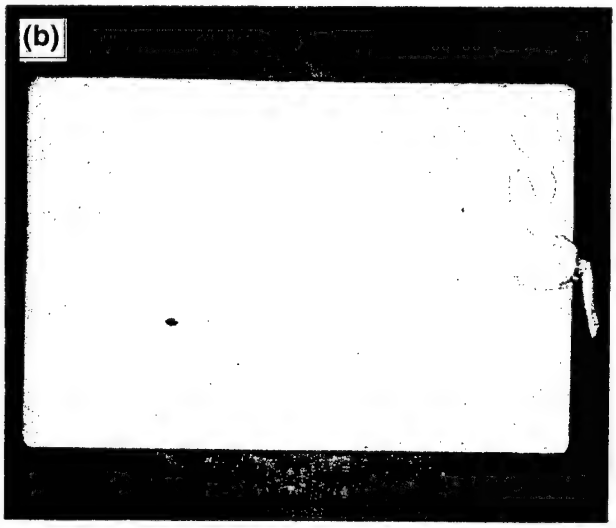

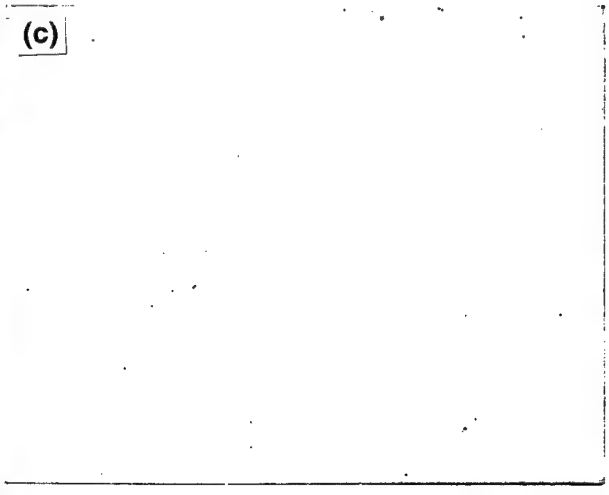

Fig. 2. Comparison of D-values calculated from f_b values and from visual rating data for (a) CR6 exposed at PH, KW, and AS, (b) CR6 in AS after 222 days (3×), and (c) CR6 in NS(PH) after 209 days (3×).

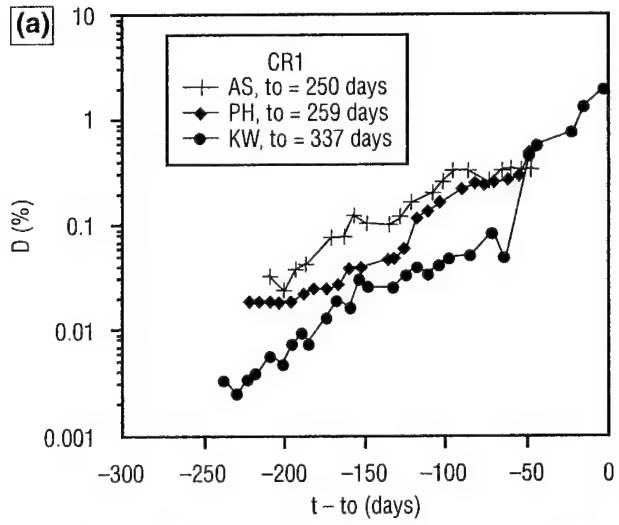

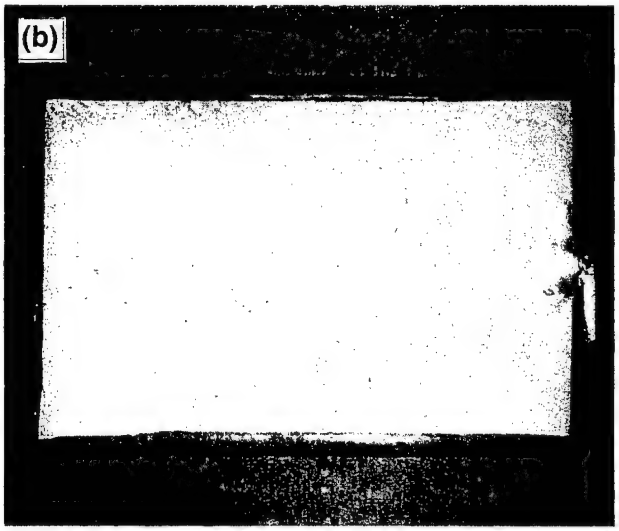

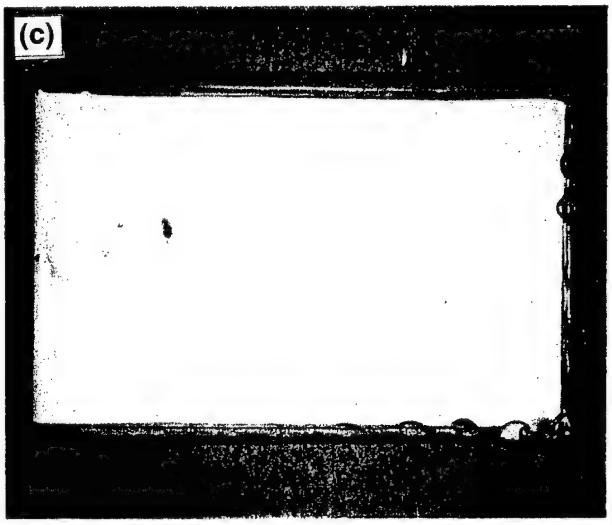

Fig. 3. Time dependence of D for CR1 exposed in (a) AS and in NS(PH and KW), (b) CR1 in AS after 225 days (3×), and (c) CR1 in NS(PH) after 278 days (3×).

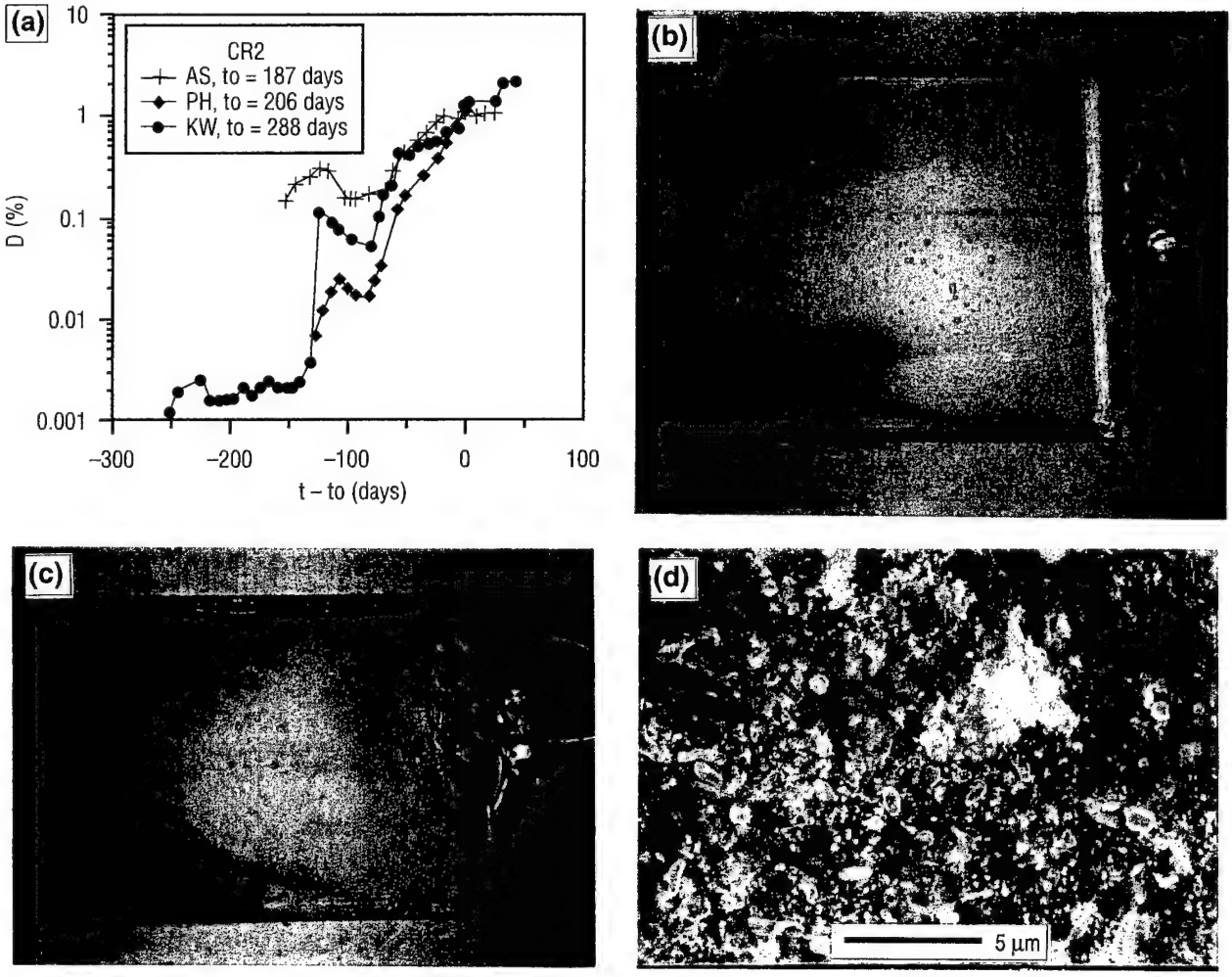

Fig. 4. Time dependence of D for CR2 exposed in (a) AS and in NS(PH and KW), (b) CR2 in AS after 415 days (1/2×), (c) CR2 in NS(PH) after 208 days (1/2×), and (d) CR2 in NS(PH) after 208 days (4000×).

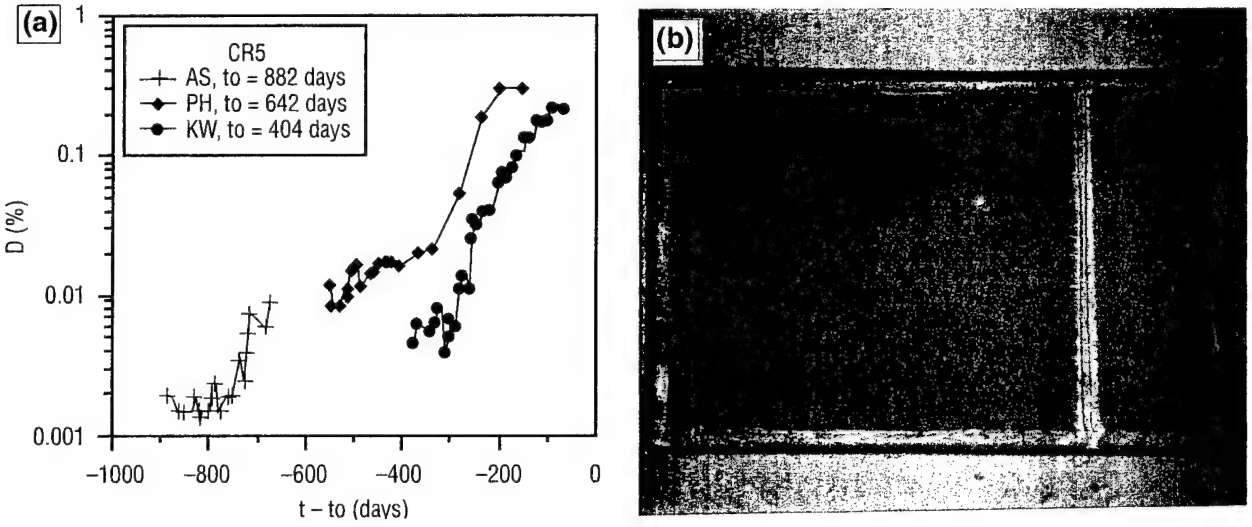

Fig. 5. Time dependence of D for CR5 exposed in (a) AS and in NS(PH and KW) and (b) CR5 in AS after 222 days (3×).

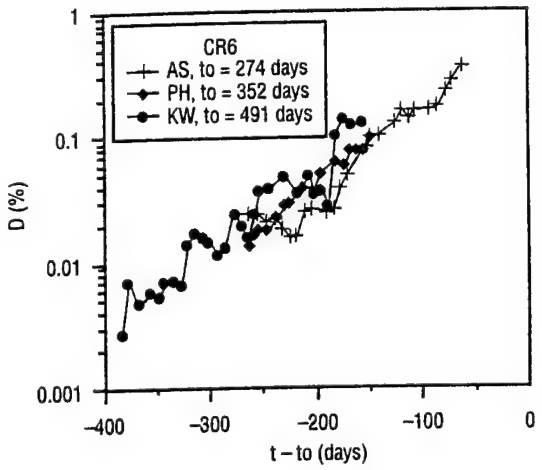

Fig. 6. Time dependence of D for CR6 exposed in AS and in NS(PH and KW).

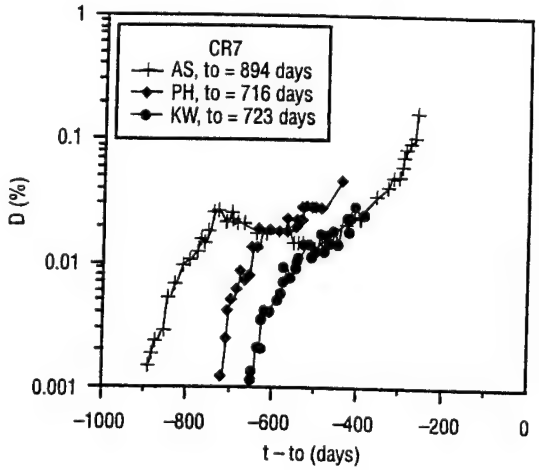

Fig. 7. Time dependence of D for CR7 exposed in AS and in NS(PH and KW).

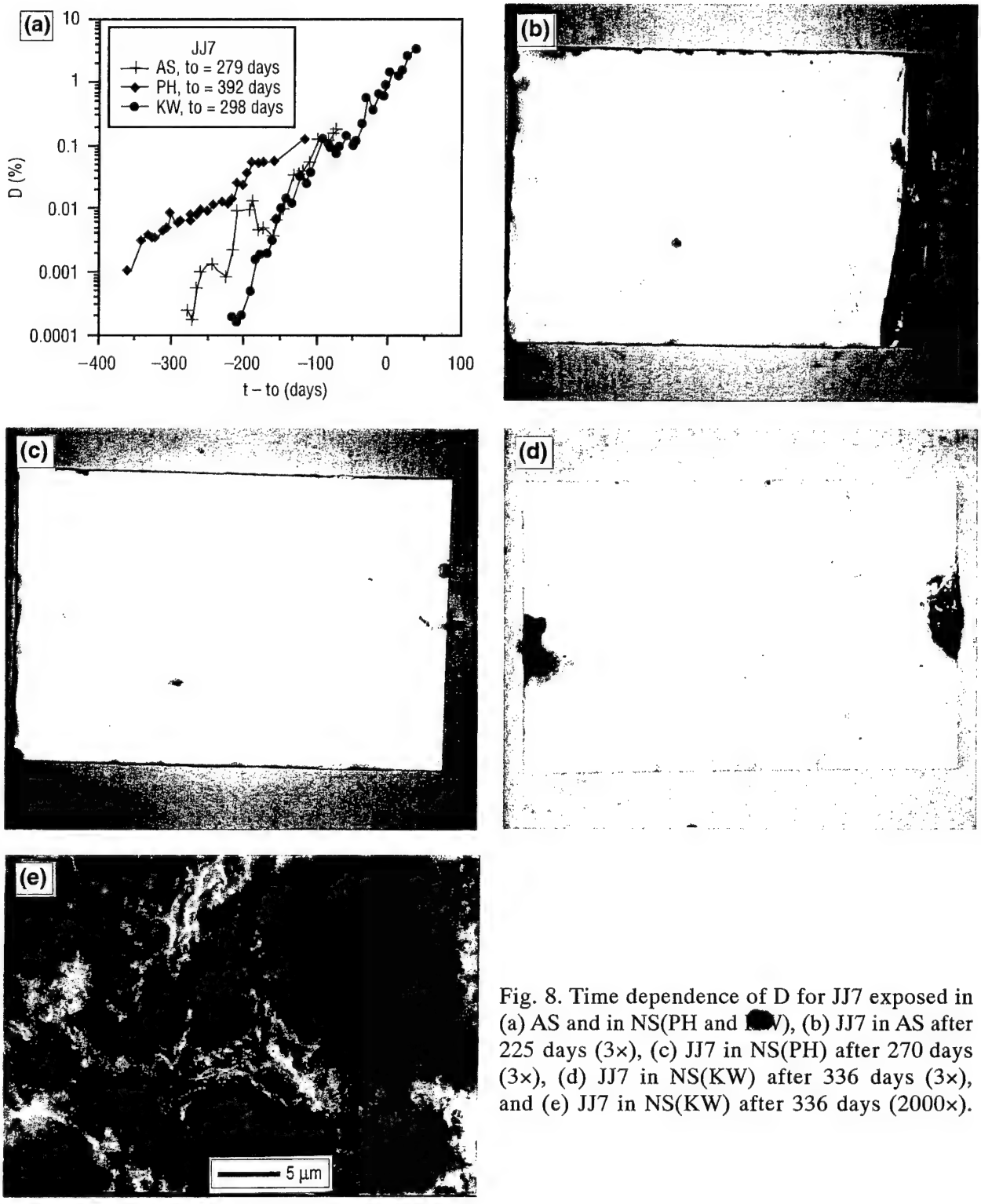

Fig. 8. Time dependence of D for JJ7 exposed in (a) AS and in NS(PH and KW), (b) JJ7 in AS after 225 days (3×), (c) JJ7 in NS(PH) after 270 days (3×), (d) JJ7 in NS(KW) after 336 days (3×), and (e) JJ7 in NS(KW) after 336 days (2000×).

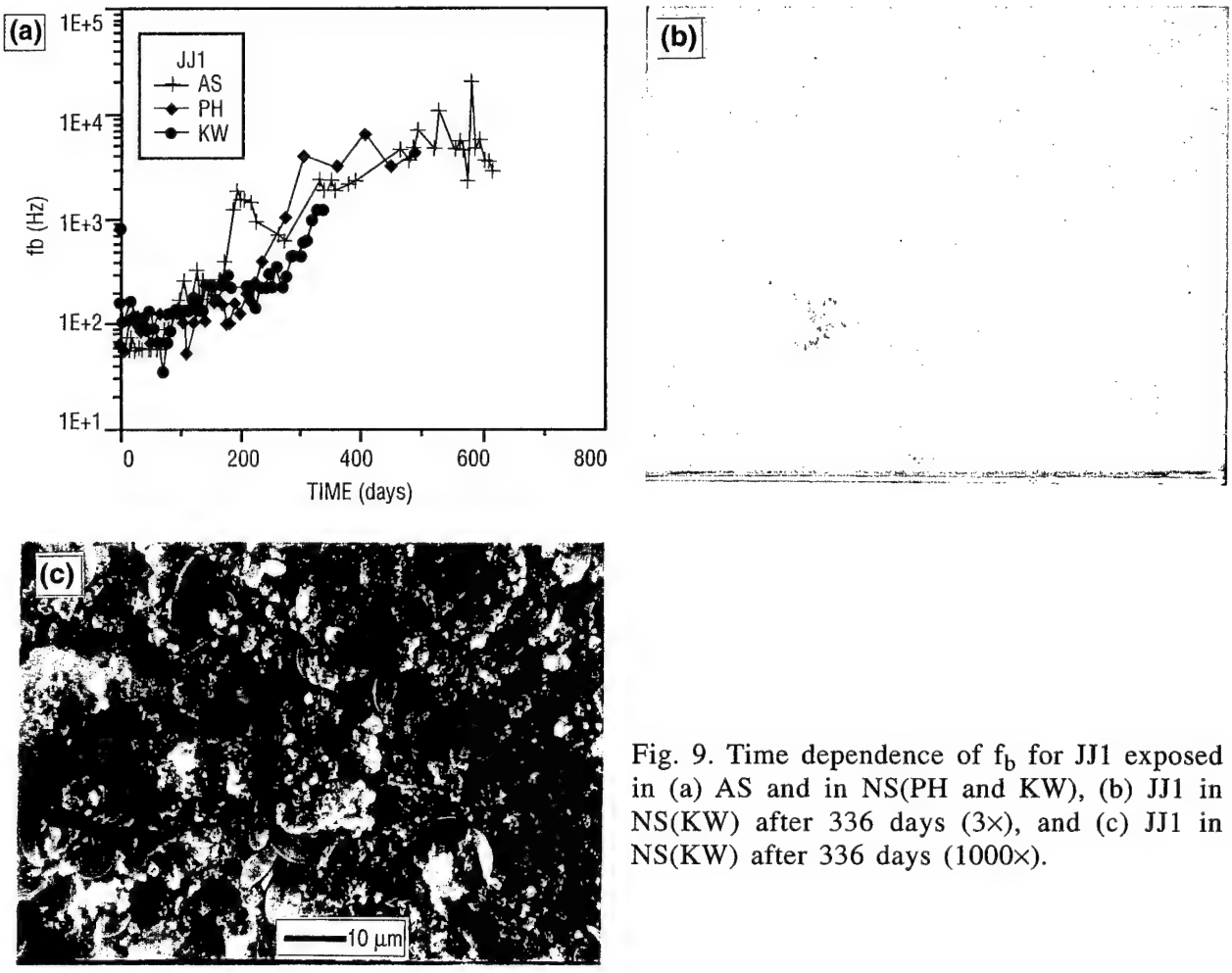

Fig. 9. Time dependence of f_b for JJ1 exposed in (a) AS and in NS(PH and KW), (b) JJ1 in NS(KW) after 336 days (3×), and (c) JJ1 in NS(KW) after 336 days (1000×).

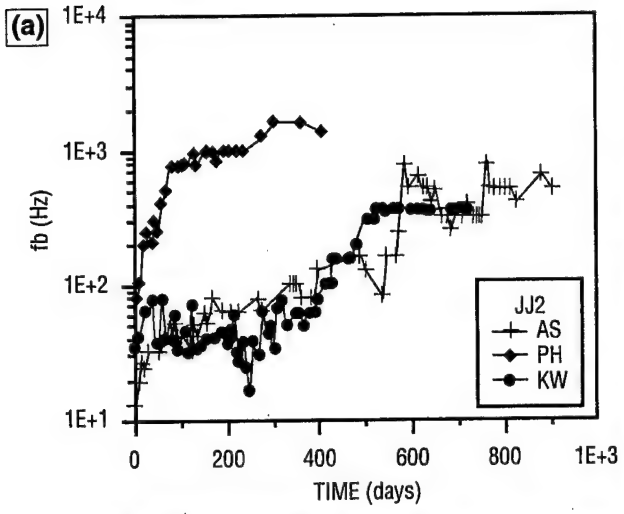

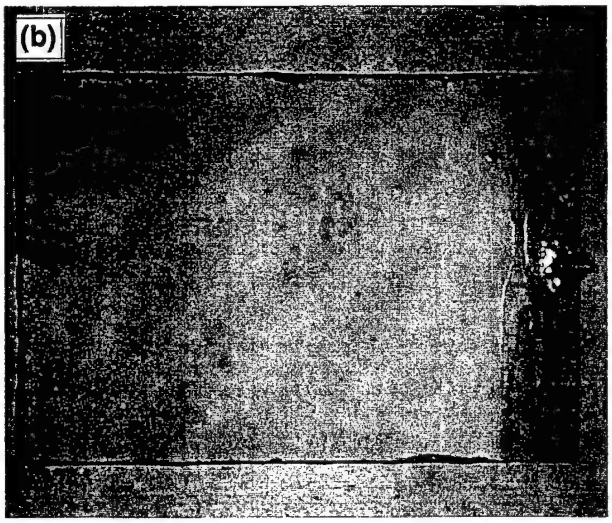

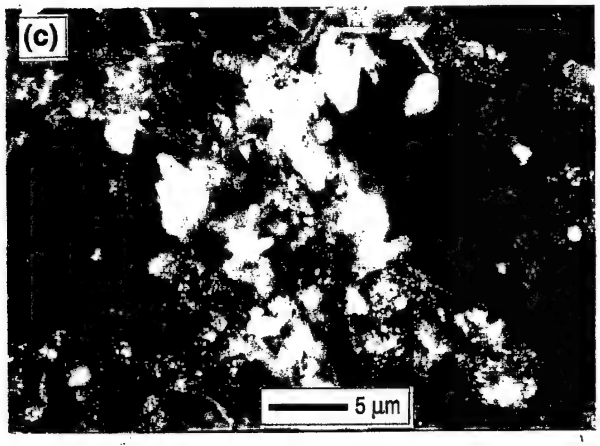

Fig. 10. Time dependence of f_b for JJ2 exposed in (a) AS and in NS(PH and KW), (b) JJ2 in NS(PH) after 405 days (3×), and (c) JJ2 in NS(PH) after 405 days (2000×).

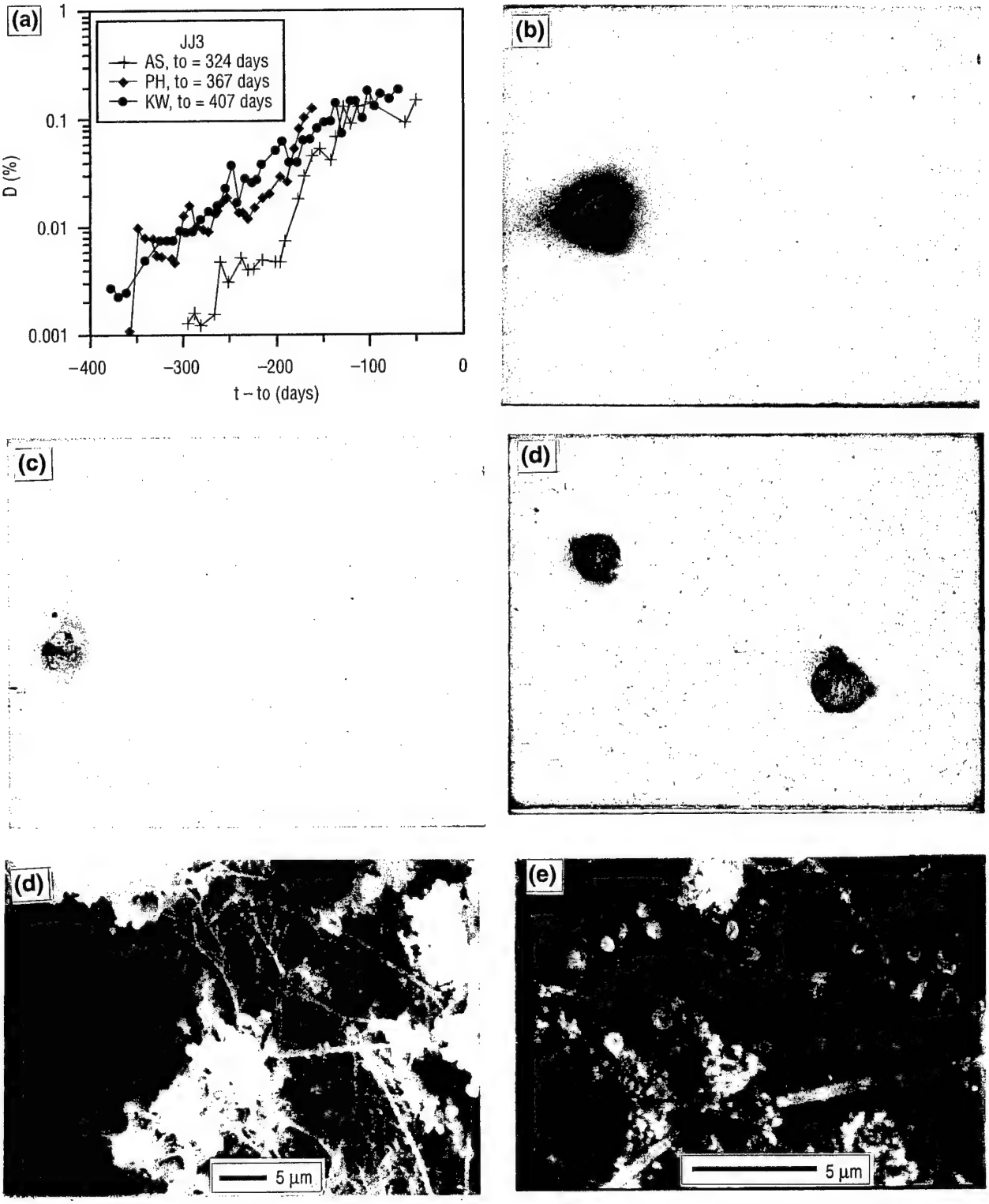

Fig. 11. Time dependence of D for JJ3 exposed in (a) AS and in NS(PH and KW), (b) JJ3 in AS after 637 days (3×), (c) JJ3 in NS(PH) after 209 days (3×), (d) JJ3 in NS(KW) after 336 days (3×), (e) JJ3 in NS(PH) after 209 days (2000×), and (f) JJ3 in NS(KW) after 336 days (4000×).

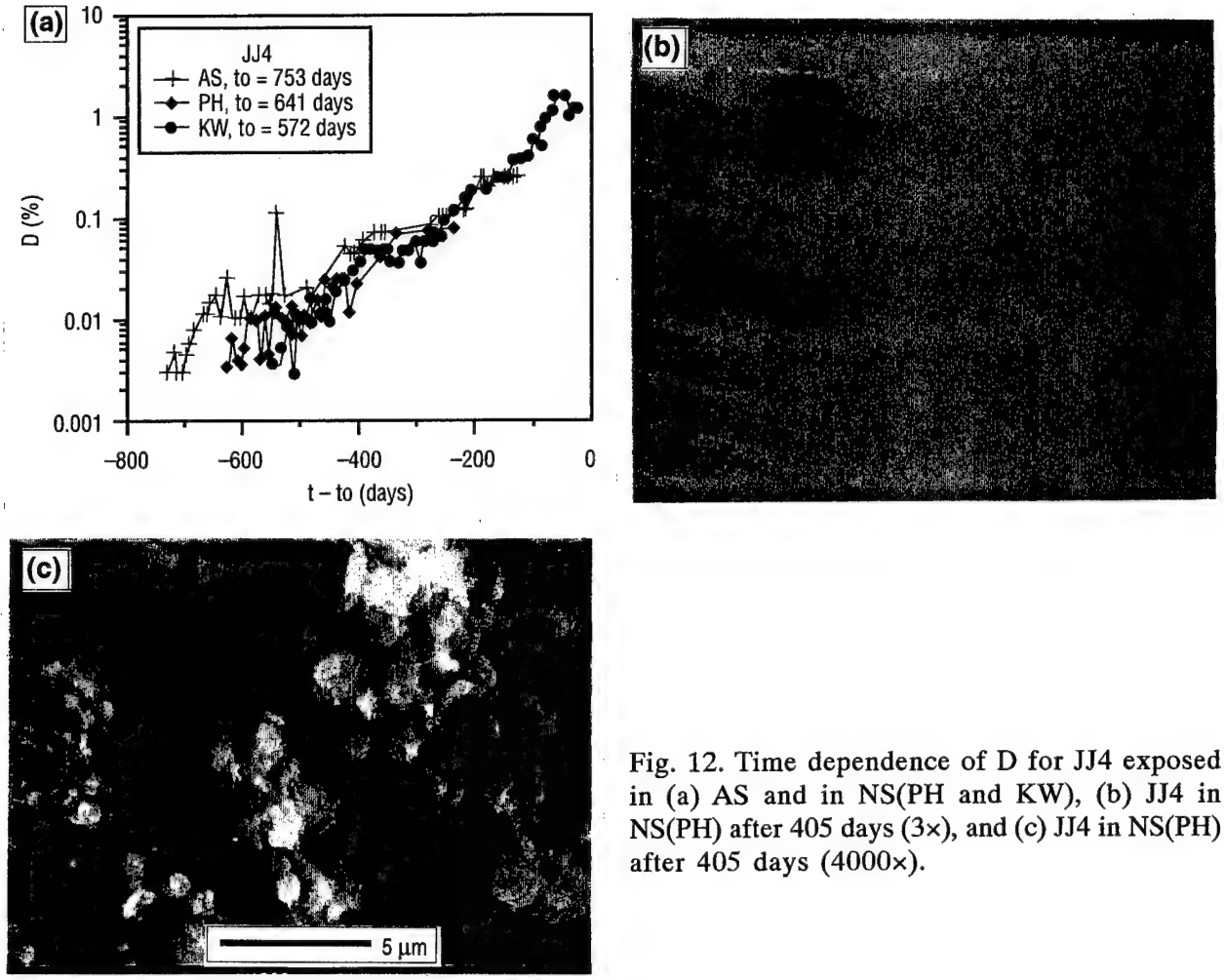

Fig. 12. Time dependence of D for JJ4 exposed in (a) AS and in NS(PH and KW), (b) JJ4 in NS(PH) after 405 days (3×), and (c) JJ4 in NS(PH) after 405 days (4000×).

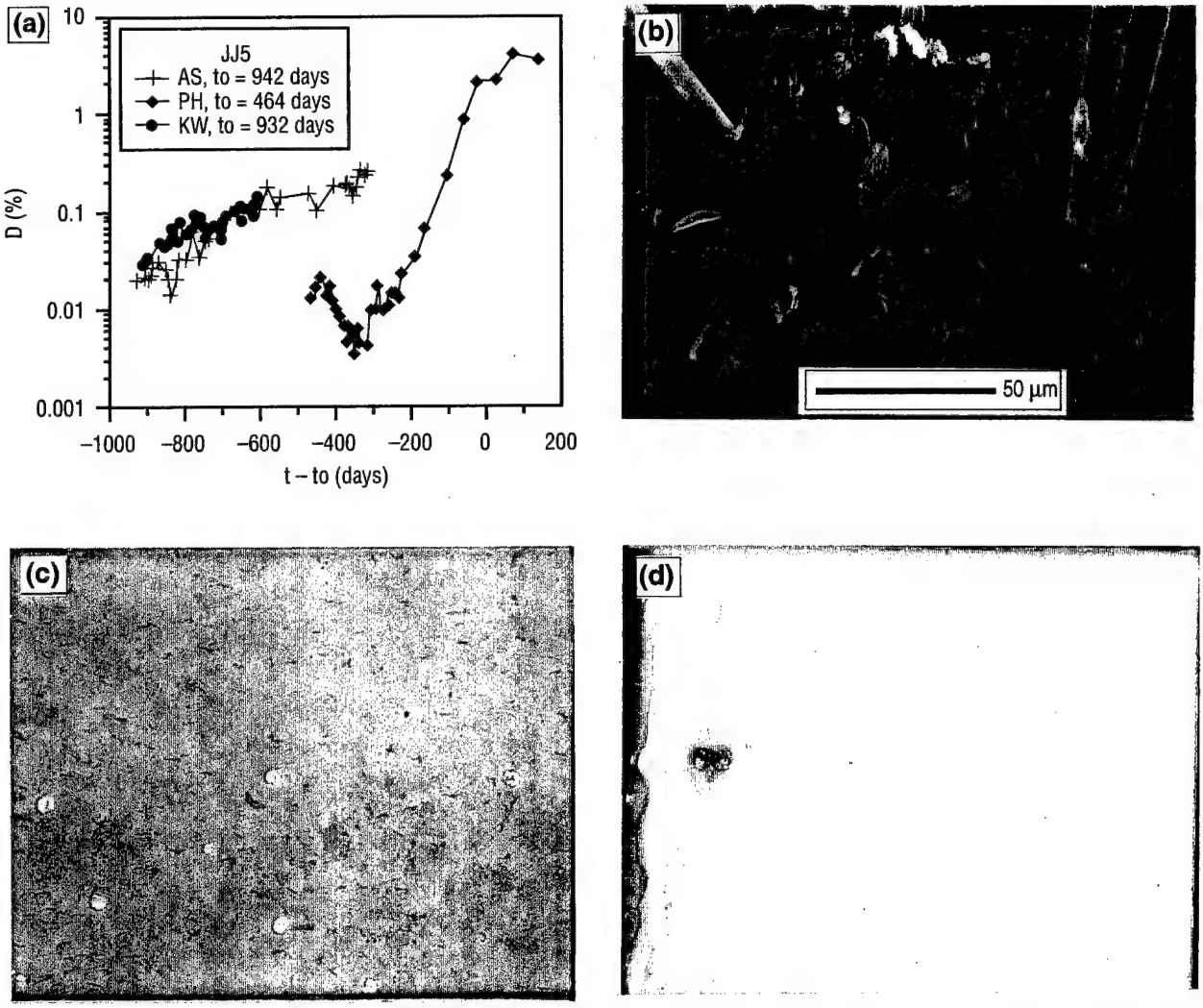

Fig. 13. Time dependence of D for JJ5 exposed in (a) AS and in NS(PH and KW), (b) JJ5 in NS(KW) after 336 days (500×), (c) JJ5 in NS(KW) after 336 days (3×), and (d) JJ5 in NS(PH) after 621 days (3×).

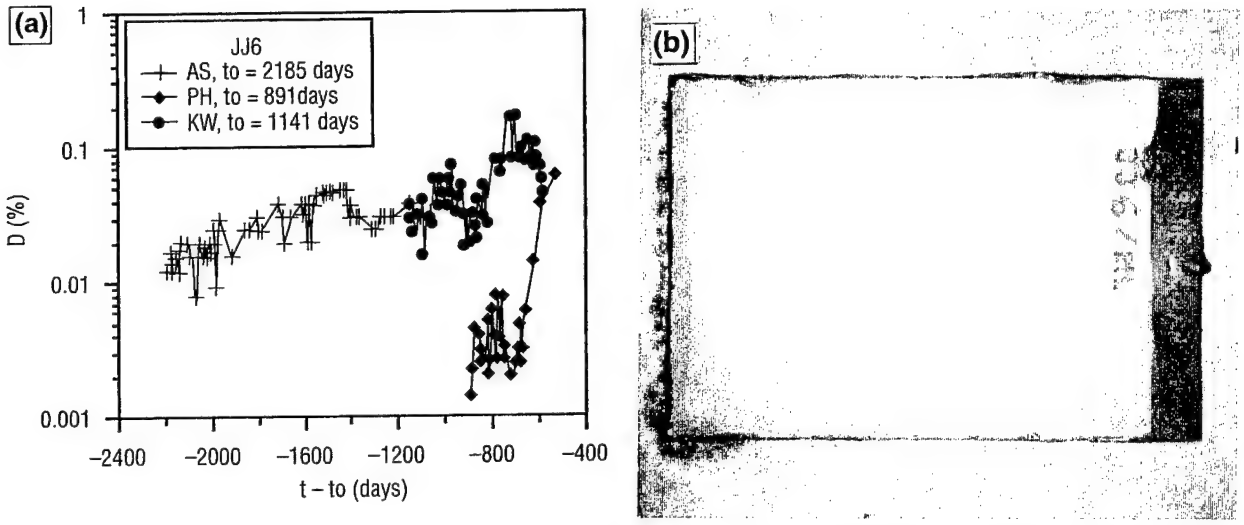

Fig. 14. Time dependence of D for JJ6 exposed in (a) AS and in NS(PH and KW) and (b) JJ6 in NS(PHH) after 621 days (3×).

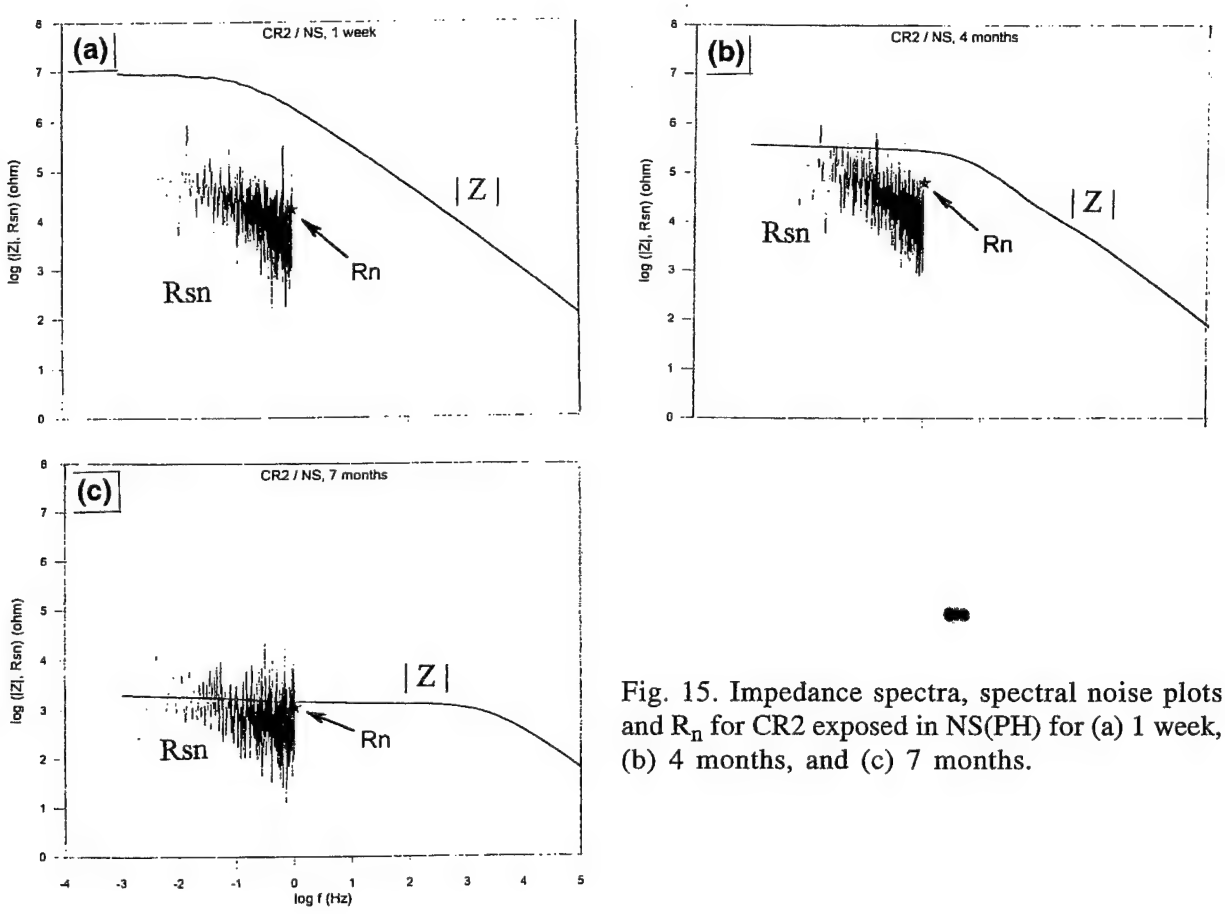

Fig. 15. Impedance spectra, spectral noise plots and R_n for CR2 exposed in NS(PH) for (a) 1 week, (b) 4 months, and (c) 7 months.

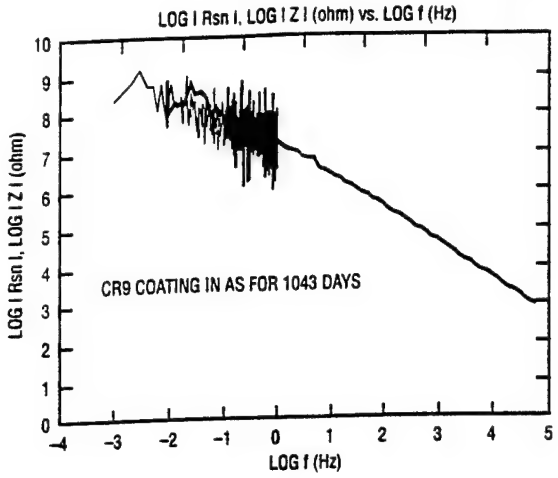

Fig. 16. Spectral noise plots and impedance spectra for CR9 exposed in AS for 1043 days.

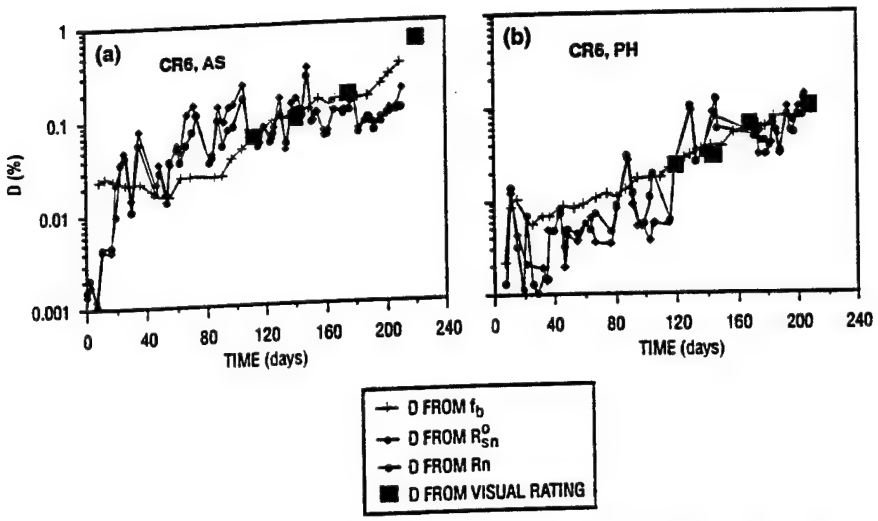

Fig. 17. Time dependence of D values obtained from f_b, R_n, and R_{sn}^o and visual observation for CR6 exposed in (a) AS and (b) NS(PH).

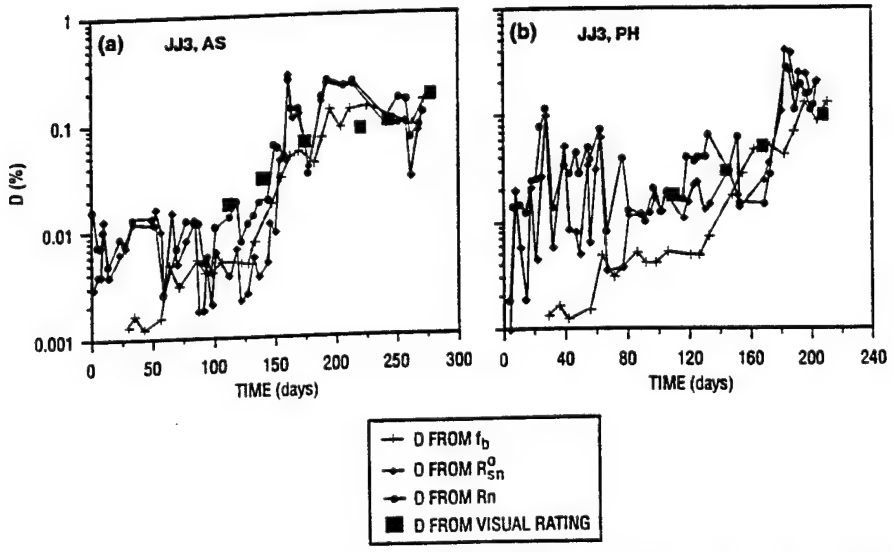

Fig. 18. Time dependence of D values obtained from f_b, R_n, and R_{sn}^o and visual observation for JJ3 exposed in (a) AS and (b) NS(PH).

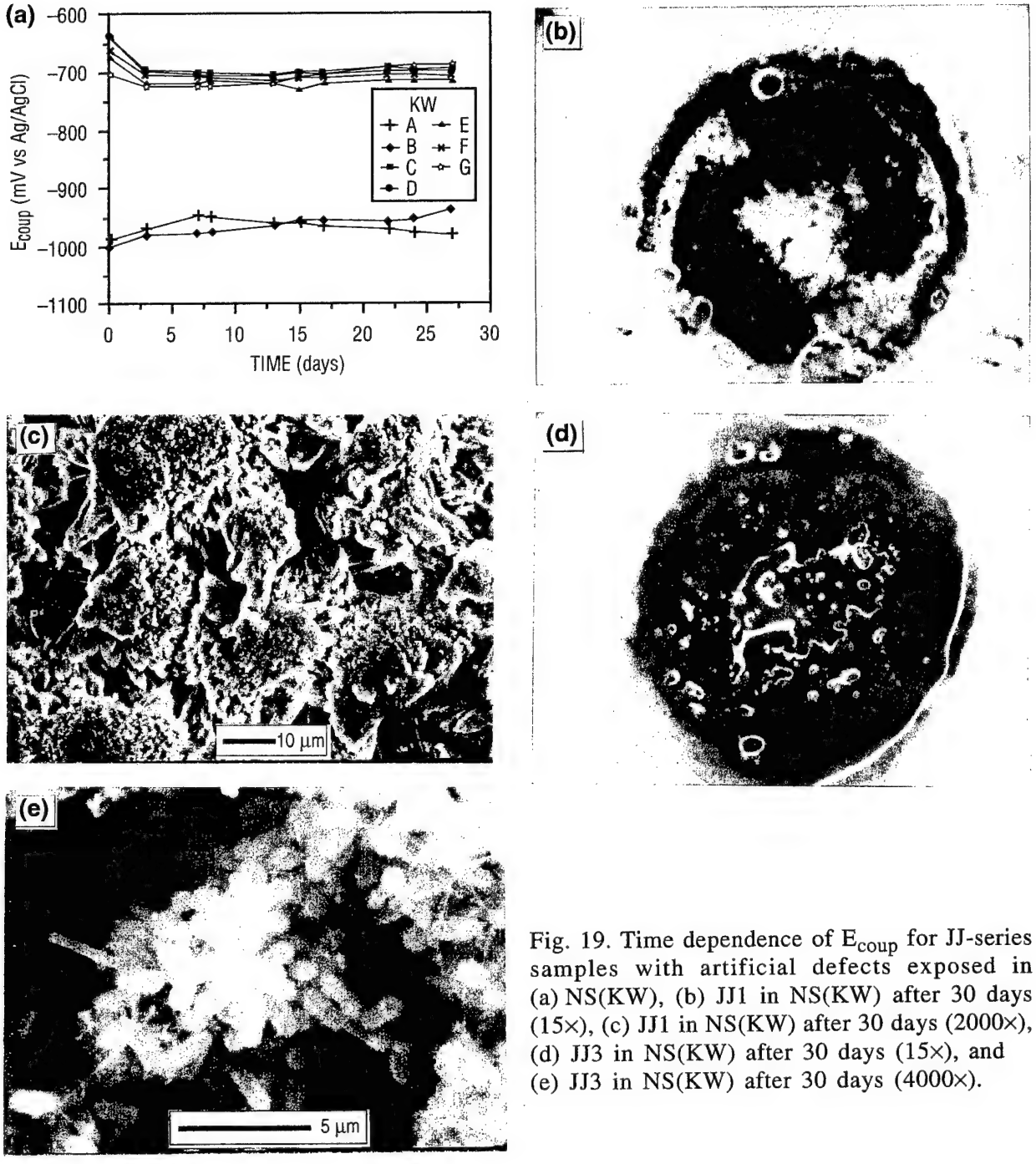

Fig. 19. Time dependence of E_{coup} for JJ-series samples with artificial defects exposed in (a) NS(KW), (b) JJ1 in NS(KW) after 30 days (15×), (c) JJ1 in NS(KW) after 30 days (2000×), (d) JJ3 in NS(KW) after 30 days (15×), and (e) JJ3 in NS(KW) after 30 days (4000×).

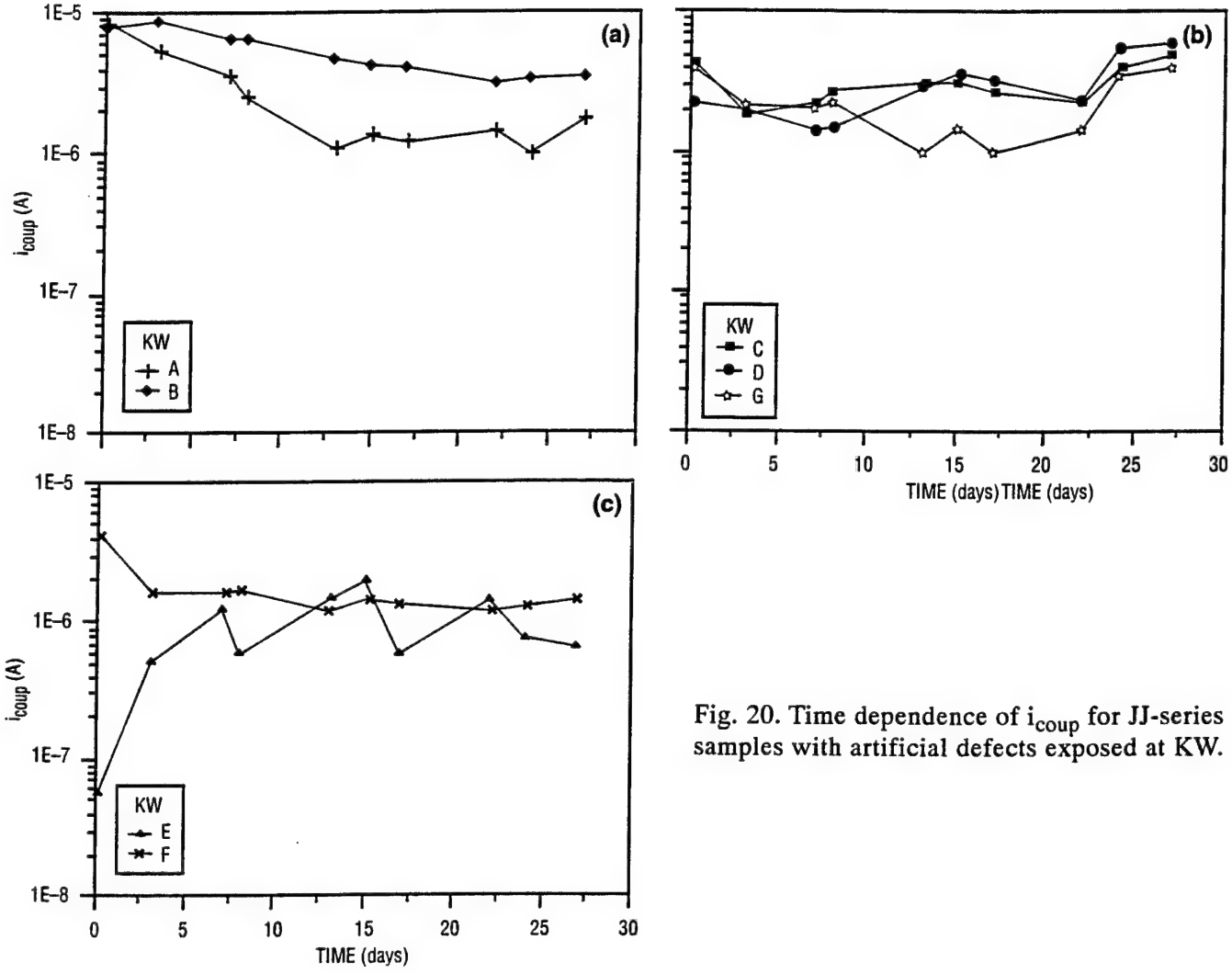

Fig. 20. Time dependence of i_{coup} for JJ-series samples with artificial defects exposed at KW.

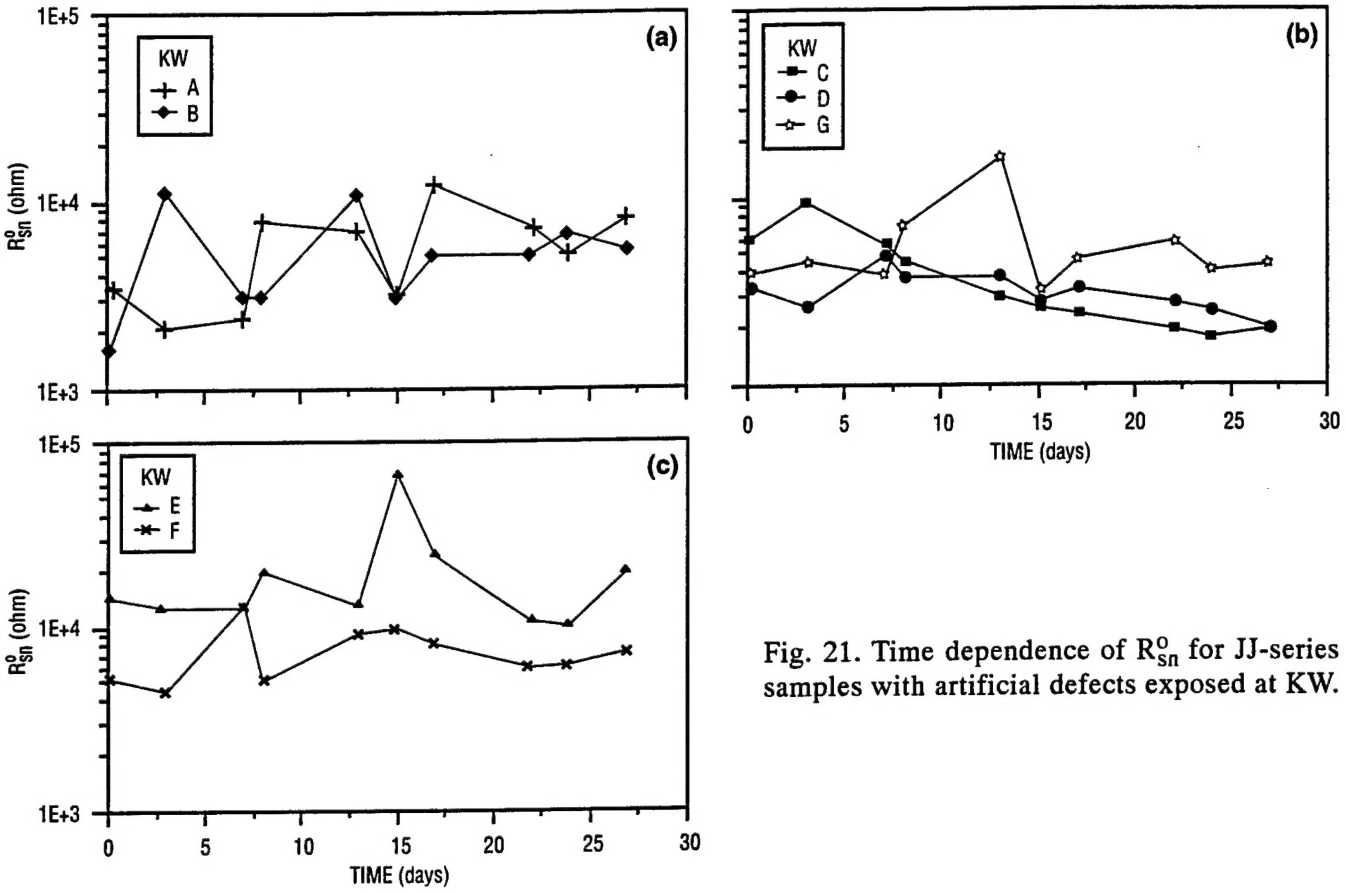

Fig. 21. Time dependence of R^o_{sn} for JJ-series samples with artificial defects exposed at KW.

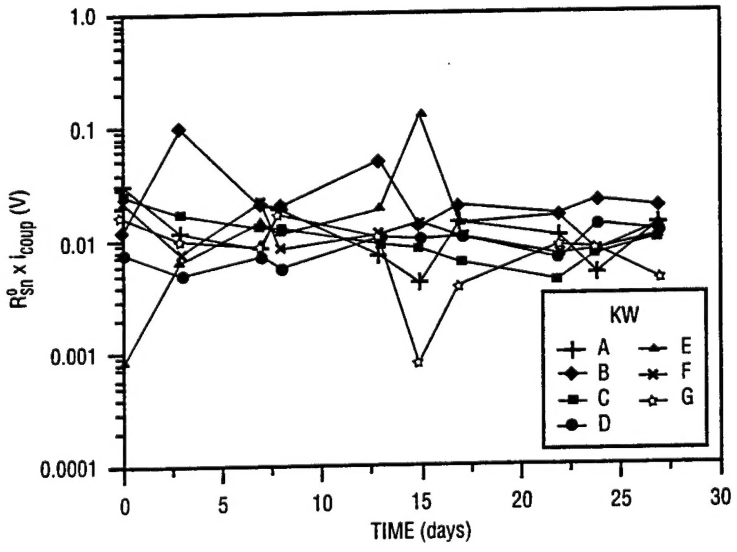

Fig. 22. Time dependence of R^o_{sn}x i_{coup} for JJ-series samples with artificial defects exposed at KW.

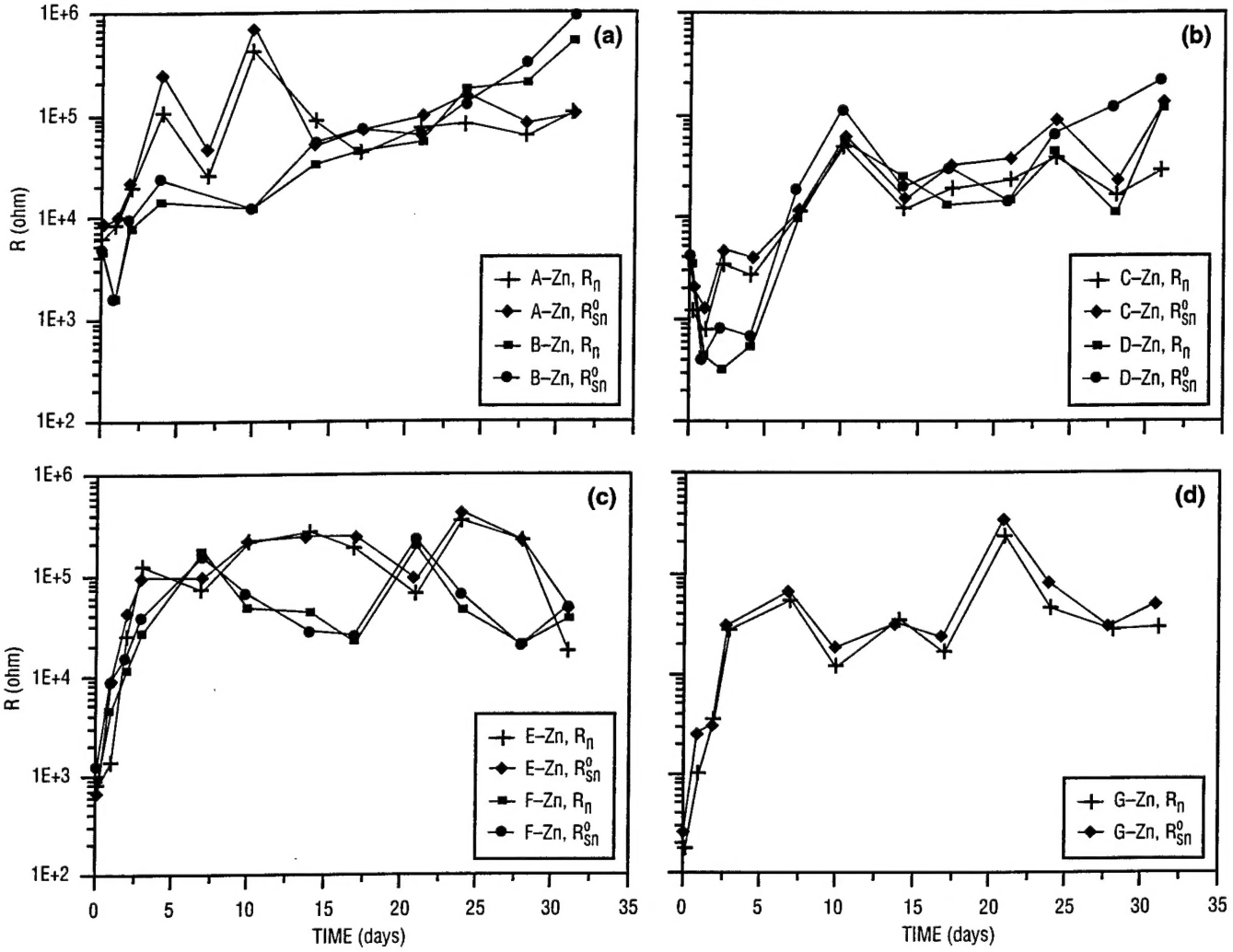

Fig. 23. Time dependence of R_n and R^o_{sn} for cathodically protected JJ-series samples with artificial defects exposed to AS.

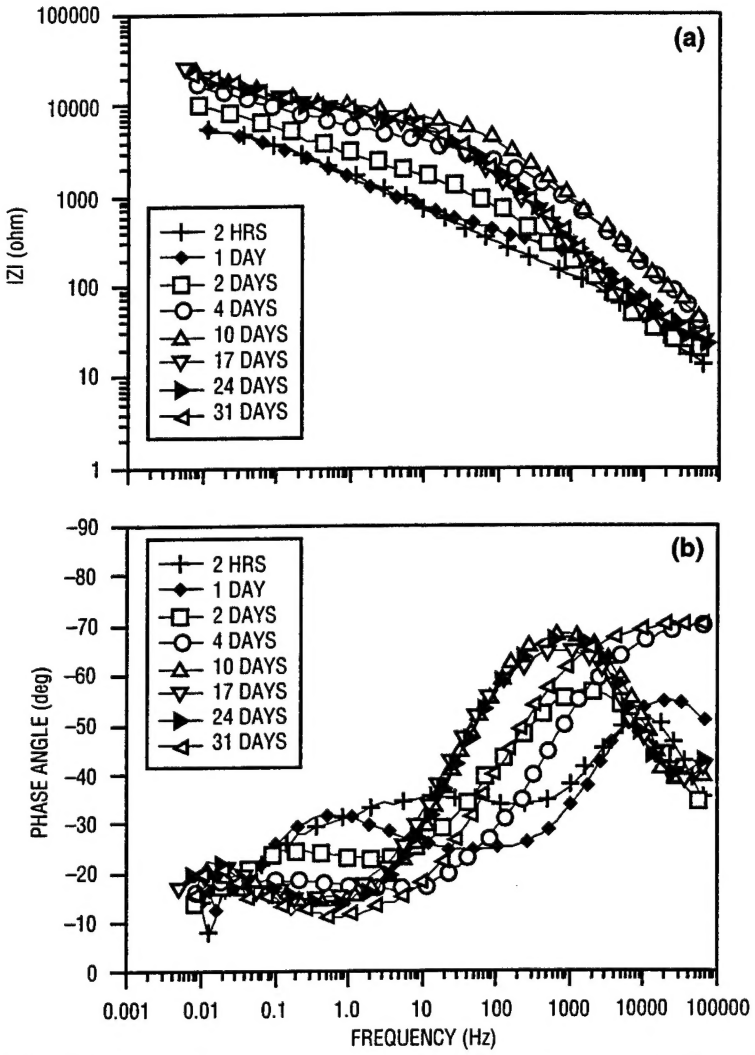

Fig. 24. Impedance spectra as a function of exposure time to AS for cathodically protected JJ5 sample with artificial defects.

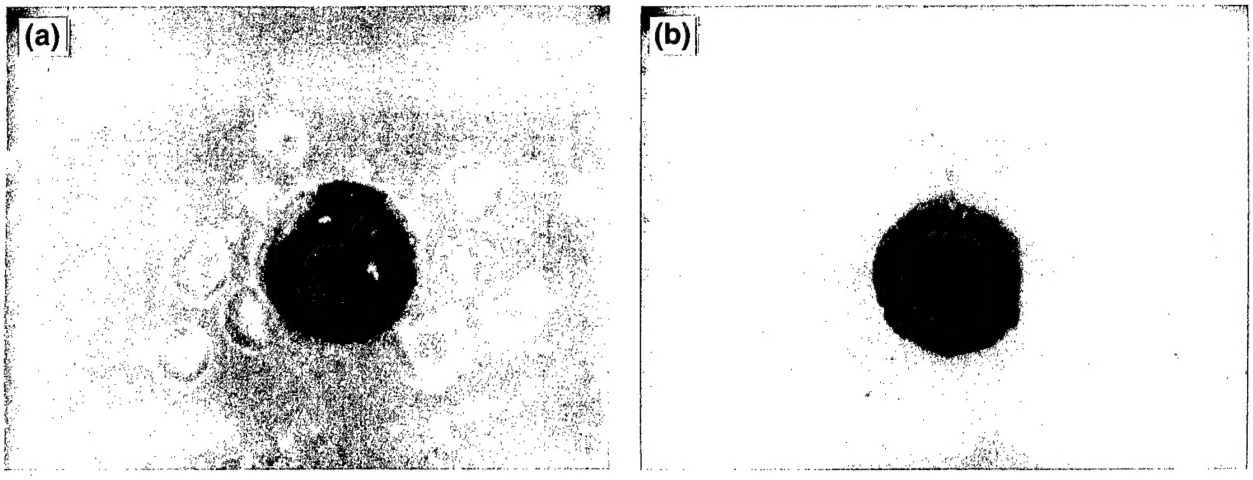

Fig. 25. Control (uninoculated) coated coupons exposed to culture medium 70 days (a) JJ3 and (b) JJ4.

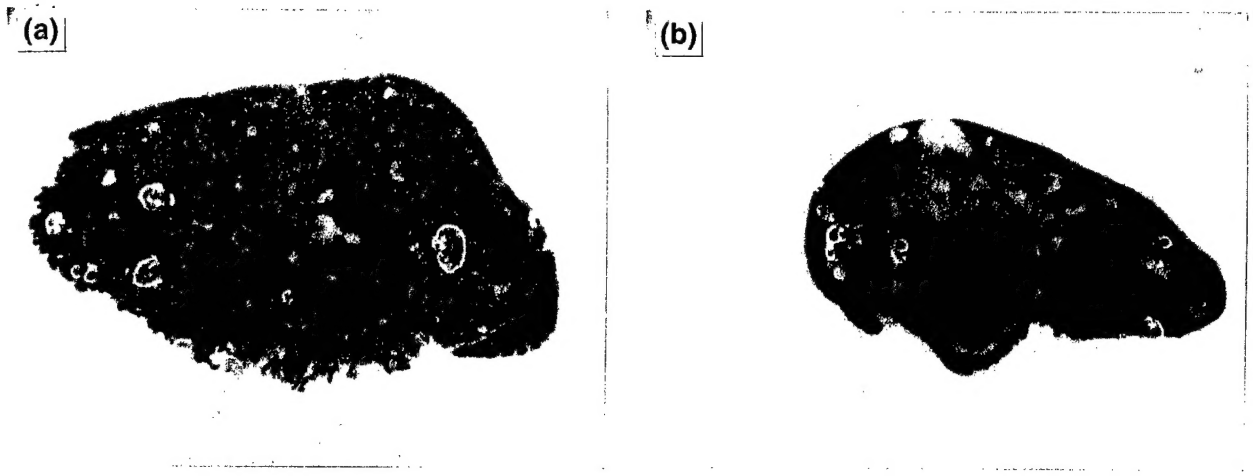

Fig. 26. Coated coupons exposed to bacterial cultures 70 days (a) JJ3 exposed to CG59 and (b) JJ4 exposed to P14.

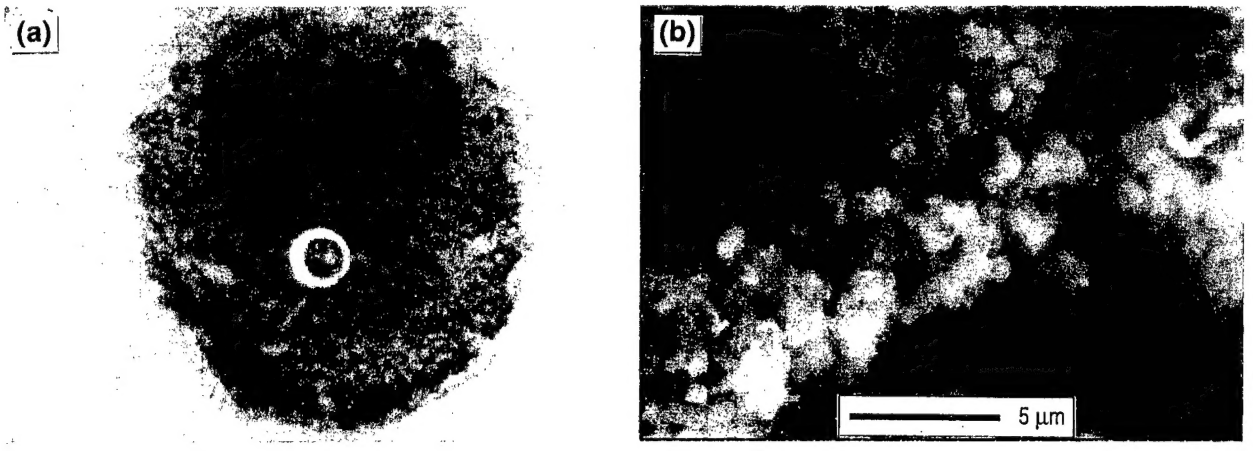

Fig. 27. JJ6 exposed to 49Z 175 days (a) 15× and (b) 4000×.